Physics – Uspekhi **60** (1) 58 – 90 (2017)

REVIEWS OF TOPICAL PROBLEMS PACS numbers: 61.05.F –, 61.66.Dk, **63.20. – e**, **75.10. – b**, 75.30.Mb, 75.40.Gb

Neutron spectroscopy and strongly correlated electrons: a view from the inside

P A Alekseev

DOI: https://doi.org/10.3367/UFNe.2016.04.037785

Contents

Abstract. Neutron spectroscopy results concerning the characteristic features of electronic states in strongly correlated electron systems are reviewed. It is shown that the effects of crystal electric field, exchange interaction, and local-itinerant electron hybridization, separately or in combination, manifest themselves in the spectral features of magnetic neutron scattering. The review discusses information that can be obtained from these spectra to be used to investigate the nature of heavy-fermion, intermediate-valence, and a number of other nontrivial types of ground states occurring in this class of systems. Problems interpreting experimental results are pointed out, suggesting the need for the development of the existing models.

Keywords: inelastic magnetic neutron scattering, rare earth intermetallic compounds, crystal electric field, magnetic ordering, heavy fermions, valence instability

P A Alekseev National Research Centre 'Kurchatov Institute', pl. Akademika Kurchatova 1, 123182 Moscow, Russian Federation; National Research Nuclear University "MEPhI", Kashirskoe shosse 31, 115409 Moscow, Russian Federation
E-mail: alekseev_pa@nrcki.ru, pavel_alekseev-r@mail.ru

Received 25 February 2016, revised 7 April 2016
Uspekhi Fizicheskikh Nauk **187** (1) 65 – 98 (2017)
DOI: https://doi.org/10.3367/UFNr.2016.04.037785
Translated by P A Alekseev

1. Introduction

Let us pose a simple question: what is the difference in the scientific output between the experimental results obtained by the diffraction and spectroscopic methods, independently from the kind of irradiation used? The short answer may be formulated as follows: from diffraction, that is, a static characteristic, we obtain information about the structural organization of matter, whereas from spectroscopy, that is, the study of the dynamics, we get information about the origin and character of the forces and interaction which determine the properties of the material, including the structure itself. The above consideration is applicable in full measure to the neutron scattering methods in condensed matter physics, to diffraction and to spectroscopy, the latter frequently being denoted as inelastic neutron scattering (INS).

What kind of questions and tasks in this respect can be formulated for studies in field of systems with strongly correlated electrons? In the most general approach, this is the study of the source of diversity in the properties and features of the ground state (that is, a manifold of the properties at temperatures approaching zero). Indeed, a specific feature of strongly correlated electron systems (SCESs) is the realization of the large variety of particular ground states: from insulator up to superconductor and from magnetically ordered to nonmagnetic states accompanied by spin fluctuation for each magnetic ion. Moreover, very different combinations of the above mentioned particular properties are possible, for instance, magnetic — superconductor.

To evaluate the role and place occupied by neutron spectroscopy in the solution of the above formulated

problem, let us consider in more detail this collection of questions.

1.1 Main problems of the physics of strongly correlated electron systems requiring microscopic consideration

What is considered to be a system with strong electron correlations? In the most general sense, it is the crystal in which the potential energy of interacting electrons is not negligible or small with respect to its kinetic energy. The important consequence of this condition is, for example, the existence of the localized magnetic moments in metals containing ions with partly unfilled (d- or f-type) orbitals. At the present time, the existence of localized magnetic moments in metals or intermetallic compounds based on transition or rare earth elements is considered a 'norm of behavior'. In fact, the beginning of the modern physics of SCESs is related to the discovery and subsequent explanation in the 1960s of the Kondo-effect, which appears to have originated from the specific interaction of conduction electrons with localized magnetic moments. The actual subjects of study at the present time are 'anomalous' systems where such moments behave 'not as must' for the local magnetic moment. That behavior is quite exotic, for instance, a magnetic moment 'disappears' (from the thermodynamic viewpoint) with a decrease in temperature, or participates in very fast spin fluctuations, or takes part in the formation of a band of very heavy electrons near the Fermi energy — so called 'heavy fermions' (HFs) with the effective mass up to hundreds of times larger than the 'normal' effective electron mass. These HFs may further interact with one another, even to the formation of superconducting pairs.

According to contemporary conceptions (which have been formed to a considerable degree based on the results of neutron studies), the manifold unusual properties of SCESs result from the coexistence and competition of the three main types of interactions intrinsic to the electronic subsystem in solids: the effects of the crystal electric field (CEF), inter-ion indirect exchange interaction, which in metals usually described by the Ruderman–Kittel–Kasuya–Yosida (RKKY) model, and hybridization of the localized (d-, f-) and itinerant (or band) electrons (denoted as c-electrons). The mutual influence and possible resulting types of ground states are schematically presented in Fig. 1.

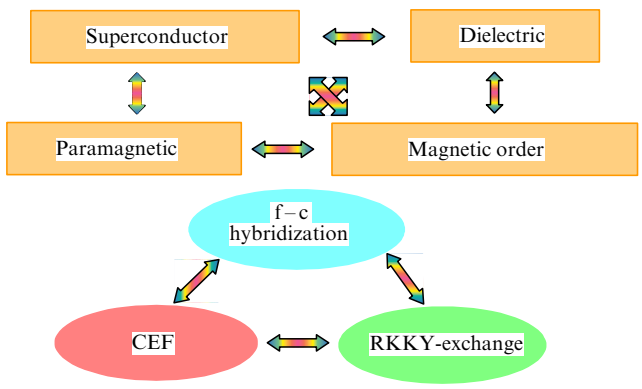

Figure 1. Three types of interaction (in ovals, below), vital for the localized moments, form different ground states (in rectangles, above); different combinations of these interactions may also be realized as shown by the arrows.

The combined result of these interactions, such as the formation of multi-particle states that originated from the scattering of one quasi-particle in solids on other quasi-particles and are dynamical in its origin, just appears as the subject of study for the physics of SCESs. It is clear that the spectroscopy methods take on special significance in this work due to the dynamical specifics of the problem.

What are the particular problems in this field which have been or are under consideration in the study started and then developed continuously during approximately the last 40 years?

The starting point was the problem of direct observation of the splitting of the ground state spin–orbit J-multiplet ($\mathbf{J} = \mathbf{L} + \mathbf{S}$) of rare earth ion (RE) f-shell (degenerate in the free state of the ion) under the influence of the CEF in the metallic matrix. Afterwards, interest was focused on the cooperative effects regarding the RKKY-interaction in the system of the magnetic moment in the periodic lattice of the rare earths for intermetallic compounds (ordered alloys).

At the beginning of the 1980s, the focus of research was concentrated on the formation of the 'heavy fermion' state for intermetallic compounds with RE ions from the beginning (Ce) and the end (Yb) of the lanthanide series, and a little later it was expanded to the 'intermediate (mixed, fluctuative, unstable) valence' system with Sm, the above mentioned Ce and Yb, and then Eu. The study of the essence and driving forces of these phenomena, its relation to the Kondo-effect approach, which is basically an impurity one in character, and conditions for transferring this concept to the periodic lattice of RE ions (Anderson model) takes on special significance.

Further on, high temperature superconductivity (HTSC) was discovered for cuprates, which appears to belong to SCESs. The question of the role of strong electron correlation in the formation of superconducting states for copper oxides, and later (in the 21st century) for iron pnictides and chalcogenides, is still relevant.

Part of the particular problems in the framework of these (and some other) tasks have been experimentally solved (for instance, the problem of huge magnetoresistance), but many of them are the subject of intensive experimental, as well as theoretical, studies to date. Among them, it is necessary to mention one of the most brilliant effects in SCES physics — connected temperature driven transitions of metal–insulator and magnetic–nonmagnetic states, which have been observed in a number of valence unstable systems united under the title 'Kondo-insulators'.

1.2 Specific features of the neutron spectroscopy method essential for studies in the field of strongly correlated systems

Methods based on neutron scattering, spectroscopy in particular (energy transfer range of $10^{-1} - 10^{-3}$ eV for the most frequently used thermal neutrons), owing to its specific features, play a special role and make a significant contribution to experimental studies in relevant areas of SCES research. This takes place in spite of the technical complexity and number of other peculiarities not in favor of this method, in contrast to the case of X-rays, for example. What are the attractive advantages of the neutron spectroscopy method?

There are several:

(1) charge neutrality, providing a high penetration capacity of neutrons with respect to electromagnetic irradiation, X-rays, and charged particles;

(2) neutrons interact not only with the nucleus but also with magnetic moments, due to specifics of the neutron spin originating magnetic moment. Comparable amplitudes of nuclear and magnetic scattering for thermal neutrons provide close values for scattering intensity (described by so-called 'scattering cross sections'), which allow the use of the same instruments to study lattice and magnetic excitations and structures;

(3) a very important feature is that the energy and wavelength of thermal neutrons are comparable to inter-atomic distances in solids and the excitation energy for quasiparticles like phonons, magnons, etc.;

(4) finally, the characteristic time $10^{-11}-10^{-13}$ s of interaction of neutrons with excitations in solids appears to be well tuned to the frequency range of spin fluctuations for SCESs with valence instability.

The last point is fundamentally important in the study of 'intermediate valence' systems, whose name originates from the experimental fact that for some compounds (generally based on Ce, Sm, Eu, Yb) the partial population of the f-shell has been observed under special external conditions (chemical composition, pressure, temperature). The intriguing fact is that the observed particular state of the f-shell appears to be dependent on the method of measurement. 'Fast' methods (X-ray absorption spectroscopy, photoelectron spectroscopy) with characteristic times on the order of $10^{-15}-10^{-17}$ s and demonstrate the coexistence of two f-shell configurations with the number of electrons differing by unit. The relatively 'slow' (characteristic times on the order of 10^{-9} s) method — isomer shift in γ-resonance (Mössbauer) spectroscopy — shows the intermediate position of the energy of γ-quanta, which correspond to a mixed electron configuration for f-electrons. Based on this observation, a conception (true in principal but considerably simplified, as appears later) was generated about the dynamical origin of the intermediate valence phenomenon, characterized by the time of inter-configuration fluctuations between 10^{-9} s and 10^{-15} s. As we can see from the above, neutron spectroscopy falls in this very interval. This fortunate fact allows neutron spectroscopy to be used for the study of corresponding effects in electron (magnetic) excitation spectra, as well as in lattice dynamics where electron–phonon interaction should also be modified.

The use of neutron scattering for the study of magnetic excitations (in the case of SCES physics, this is CEF effects on the initial stage of studies) is based on the magnetic dipole interaction between neutron spin and the localized magnetic moment. The result (for an unpolarized neutron beam) can be presented by the double differential cross section for neutron scattering, as was shown in [1, 2]:

$$\frac{\mathrm{d}^2\sigma}{\mathrm{d}E\,\mathrm{d}\Omega}=\frac{1}{2\pi}\left(\frac{\gamma r_\mathrm{e}}{\mu_\mathrm{B}}\right)^2 N\frac{k_\mathrm{f}}{k_\mathrm{i}}\,\chi''(\mathbf{Q},E,T)\,\frac{1}{1-\exp\left[-E/(k_\mathrm{B}T)\right]}\,, \tag{1}$$

where $\gamma=-1.91$ is the gyromagnetic ratio for a neutron, $r_\mathrm{e}=e^2/(m_\mathrm{e}c^2)$ is the classical radius for an electron, $\mu_\mathrm{B}=e\hbar/(mc)$ is the Born magneton, $\mathbf{k}_\mathrm{i}$ is the wave vector for an incoming neutron, $\mathbf{k}_\mathrm{f}$ is the wave vector for a scattered neutron, $\mathbf{Q}=\mathbf{k}_\mathrm{i}-\mathbf{k}_\mathrm{f}$ is the momentum transfer from a neutron to the sample, E is the energy transfer from a neutron to the sample, $\chi''(\mathbf{Q},E,T)\equiv\mathrm{Im}\,(\chi(\mathbf{Q},E,T))$ is the imaginary part of the dynamical magnetic susceptibility (related to RE-ion), and k_B is the Boltzmann constant.

According to the Kramers–Kronig relation $\chi''(\mathbf{Q},E,T)$ may be presented using a real part of the dynamical magnetic susceptibility $\chi'(\mathbf{Q},0,T)\equiv\mathrm{Re}\,(\chi(\mathbf{Q},E,T))$:

$$\chi''(\mathbf{Q},E,T)=E\pi\sum_{n,m}\chi'_{nm}(\mathbf{Q},0,T)\,P_{nm}(E,T)\,, \tag{2}$$

where $\chi'_{nm}(\mathbf{Q},0,T)$ is the Van-Vleck susceptibility, related to the transition between two states of local moment $|n\rangle$ and $|m\rangle$ (if $n=m$, it corresponds to the Curie susceptibility for the state $|n\rangle$), $\sum_{n,m}\chi'_{nm}(\mathbf{Q},0,T)=\chi'(\mathbf{Q},0,T)$; each function $P_{nm}(E,T)$ has a singularity (peak) with the maximum at the energy $E=E_m-E_n$, where E_n and E_m are the energies of RE-ions in the states $|n\rangle$ and $|m\rangle$, respectively, with normalization:

$$\int_{-\infty}^{+\infty}P_{nm}(E,T)\,\mathrm{d}E=1\,. \tag{3}$$

In the absence of the inter-ion interaction, the dependence $\chi'(\mathbf{Q},0,T)$ on $\mathbf{Q}$ is described by the single-ion magnetic dipole form factor $F(\mathbf{Q})$; therefore:

$$\chi'(\mathbf{Q},0,T)=\big(F(\mathbf{Q})\big)^2\,\chi'(0,0,T)\equiv\big(F(\mathbf{Q})\big)^2\chi_\mathrm{st}(T)\,, \tag{4}$$

where χ_st is the static magnetic susceptibility, which is measured in classical magnetometers.

Thus, from (1) we obtain

$$\frac{\mathrm{d}^2\sigma}{\mathrm{d}E\,\mathrm{d}\Omega}=\frac{1}{2}\left(\frac{\gamma r_\mathrm{e}}{\mu_\mathrm{B}}\right)^2\frac{k_\mathrm{f}}{k_\mathrm{i}}\big(F(\mathbf{Q})\big)^2 \times\left(\sum_{n,m}\chi'_{nm}(0,0,T)P_{nm}(E,T)\right)\frac{E}{1-\exp\left[-E/(k_\mathrm{B}T)\right]}\,. \tag{5}$$

If we assume for simplicity that $P_{nm}(E,T)$ can be presented by a succession of δ-functions, expression (5) may be transformed [1, 3] into the form

$$\frac{\mathrm{d}^2\sigma}{\mathrm{d}E\,\mathrm{d}\Omega}=(\gamma r_\mathrm{e})^2\frac{k_\mathrm{f}}{k_\mathrm{i}}\big(F(\mathbf{Q})\big)^2 \times N\sum_{n,m}\rho_n\big|\langle m|\hat{\mathbf{G}}_\perp|n\rangle\big|^2\delta\big(E-(E_m-E_n)\big)\,, \tag{6}$$

where

$$\rho_n=\exp\left(-\frac{E_n}{k_\mathrm{B}T}\right)\left[\sum_i\exp\left(-\frac{E_i}{k_\mathrm{B}T}\right)\right]^{-1}\,,$$

is the probability of finding at a given temperature the RE-ion in the state $|n\rangle$, and

$$\hat{\mathbf{G}}_\perp(\mathbf{Q})\equiv\frac{1}{Q^2}\left[\mathbf{Q}\times[\hat{\mathbf{G}}\times\mathbf{Q}]\right]$$

is an operator for the interaction of a neutron with the RE-ion,

$$\hat{\mathbf{G}}=\frac{1}{2}\,\hat{\mathbf{L}}+\hat{\mathbf{S}}\,. \tag{7}$$

When states $|n\rangle$ and $|m\rangle$ belong to the same spin–orbit J-multiplet,[1] the operator $\hat{\mathbf{G}}$ may be presented using the

[1] When the initial and final states belong to different multiplets, the matrix element for $\mathbf{G}$ and the form factor have a special form [3].

operator of the total moment of the f-shell:

$$\hat{\mathbf{G}} = \frac{1}{2}\, g_J\, \hat{\mathbf{J}}\,, \tag{8}$$

where

$$g_J = 1 + \frac{J(J+1) - S(S+1) - L(L+1)}{2J(J+1)}$$

is the Lande factor.

After the above transformation, the expression for the double differential scattering cross section (6) for the RE-ion in the CEF takes the form

$$\frac{\mathrm{d}^2\sigma}{\mathrm{d}E\,\mathrm{d}\Omega} = (\gamma r_\mathrm{e})^2 \frac{k_\mathrm{f}}{k_\mathrm{i}} \big(F(\mathbf{Q})\big)^2 \times N \sum_{n,m} \rho_n \big|\langle m|\hat{\mathbf{J}}_\perp|n\rangle\big|^2 \delta\big(E - (E_m - E_n)\big)\,. \tag{9}$$

It is necessary to mention that frequently, for the presentation of the neutron spectra, the so-called scattering function (or spectral scattering function) $S(\mathbf{Q}, E)$ is used, which is connected to the double differential scattering cross section as

$$\frac{\mathrm{d}^2\sigma}{\mathrm{d}\Omega\,\mathrm{d}E} = \frac{k_\mathrm{f}}{k_\mathrm{i}}\, S(\mathbf{Q}, E, T)\,. \tag{10}$$

The convenience of using a scattering function instead of a double differential cross section originates from the fact that just the scattering function depends directly on the spectral properties of the system under study, its temperature, momentum and energy transfer obtained from scattered neutrons. According to Eqns (2), (6), and (9), $S(\mathbf{Q}, E)$ is a combination of peaks at energies defined by the difference between energies of state coupled by allowed magnetic dipole transitions. Transition probabilities which define the intensity of the scattering are proportional to the square of the matrix element modulus $\hat{\mathbf{G}}_\perp(\mathbf{Q})$, thus being directly related to the form of the wave function corresponding to the above mentioned states. As a result, the spectrum of magnetic neutron scattering contains information on the energy and wave functions of f-electron states.

Usually, experimental spectra for a system with an f-electron J-multiplet split by a CEF are interpreted based on Eqn (9) or (5), depending on the particular system — its relaxation characteristics and the extent of cooperative interaction between magnetic ions.

It is necessary to mention two important conservation laws that are realized for the spectral function $S(\mathbf{Q}, E, T)$. The first is the principal of detailed balance, which means the energy integral over the spectrum is a constant value. The consequences are as follows. At $T \to \infty$, the spectral parts for neutron energy loss and for neutron energy gain possess equal intensity, but at $T \to 0$ all the intensity is collected in the neutron energy loss part, which in the following is considered positive energy transfer. The second is that the above considered integral (of course taking into account the elastic and quasielastic magnetic intensity, if any) after the normalization to $Q = 0$ and integration over a solid angle appears to be equal to the total magnetic scattering of the RE-ion defined by the square of the magnetic moment M^2, according to the equation

$$\sigma_\mathrm{mag} = (0.917)\left[\frac{2}{3}\, M^2\right] = (0.917)\left[\frac{2}{3}(g_J)^2 J(J+1)\right]. \tag{11}$$

Quantitatively this relationship can be characterized by an estimation: $M^2 \approx (1{,}3\mu_\mathrm{B})^2$ provides the value $\sigma_\mathrm{mag} \approx 1$ barn. It is necessary to note that typical values of the magnetic moments for the ground multiplets of RE-ions are in the range $(1-10)\,\mu_\mathrm{B}$; therefore, the scale of the values of magnetic cross sections is close to the scale of the nuclear ones. This fact provides the opportunity to use for neutron spectroscopy studies of f-electron excitation the same experimental techniques which have been designed for spectroscopy of atomic vibrations (phonon spectroscopy).

As an example illustrating the above consideration of the relationship between measured spectra and crystal field splitting, results are presented below for the paramagnetic system $PrAl_3$ which we have studied. Spectra obtained in the 1980s jointly with A Murani (ILL) using one of the best time-of-flight spectrometers at that time for thermal neutrons (IN4 at ILL) at two temperatures are shown in Fig. 2. On the left of Fig. 2a the splitting scheme (total splitting about 15 meV) determined in our previous work for Pr^{3+} is shown (see Section 2.1), being entirely confirmed in this particular experiment.

The incoming neutron energy of 12 meV allows observing a signal in the range of neutron energy loss (positive energy transfer) along with the neutron energy gain part. The detail balance principle defines the relationship between intensities in these parts. It is easy to see that, when the temperature (6 K) is much lower than the splitting between the first excited Γ_6 and ground state singlet Γ_1 ($E = 4.5$ meV$\sim$ 50 K), only one inelastic peak survives in the spectrum which corresponds to

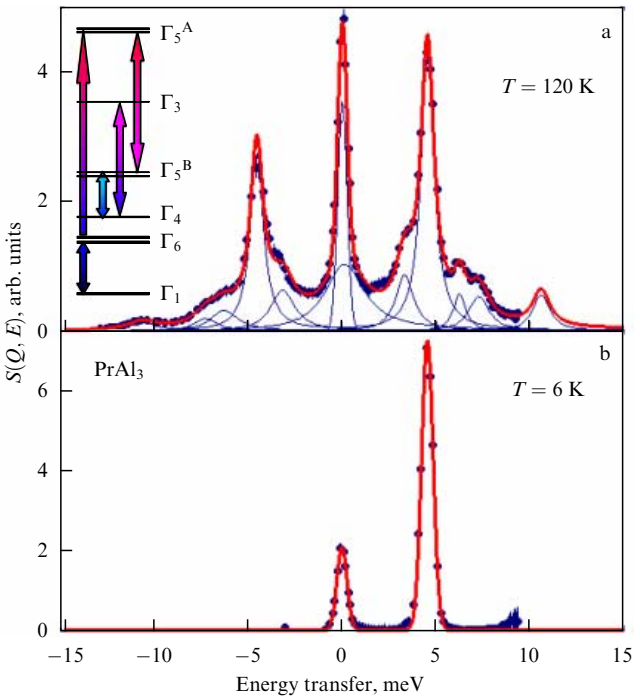

Figure 2. Spectra of inelastic neutron scattering (scattering functions) for polycrystalline $PrAl_3$ measured for a scattering angle of 15° and incoming neutron energy $E_0 = 12$ meV on the IN4 spectrometer at ILL (Grenoble) at temperatures of 120 K (a) and 6 K (b). On the left, the CEF splitting scheme is shown (arrows indicate allowed dipole transitions) which was used for calculations of $S(Q, E)$ by use of Eqn (9). The results of the calculations are presented by thin lines (separated transitions with the width defined by experimental resolution); the solid line corresponds to their sum, which includes the approximation of the elastic ($E = 0$) incoherent nuclear scattering (at low temperatures).

the transition $\Gamma_1 - \Gamma_6$, which is only allowed from the ground state. This means that the total magnetic scattering related to the magnetic moment of Pr^{3+} [in accordance with Eqn (11), for Pr^{3+} it is of the order of 7 barn] is concentrated in this particular excitation (due to the singlet ground state, there is no elastic and quasielastic scattering at this temperature). Due to this, the inelastic magnetic peak appears even more intensive than the incoherent nuclear elastic one at zero energy transfer [$\sigma_{inc}(PrAl_3) \sim 0.04$ barn]. The significant intensity of this magnetic inelastic peak in the scattering function at low temperatures gives rise to the application of the Pr^{3+} ion as a 'sensor' of CEF potential in $REAl_3$-type systems (where *RE* is a rare earth element) without disturbing the electronic subsystem of the material due to the opportunity to use a very low (around 3%) concentration of the Pr ion in the RE-sublattice (see Section 3.1).

Now, let us turn to a short review of the primary results obtained by the application of neutron spectroscopy methods in the considered field of the study.

2. Studies of the role of the crystal field and exchange interaction effects in the formation of the ground state for rare earth-based intermetallic and other compounds

2.1 Effects of crystal fields and thermodynamic properties

The fundamental effect of strong electron correlation in metals is the existence of stable magnetic moments localized on ions with partly unfilled electron shells. These moments (i) being systematically located in the crystal, interact with one another, (ii) originating from f- (or d-) shells, are subjected to the influence of the spatially inhomogeneous electrostatic potential induced by the surrounding ions if this potential really exists in a metallic substance.

This last point was considered far from trivial in the 1960s and 1970s. At that time, current studies of RE-intermetallics showed that temperature dependences of the magnetic, thermal, and transport properties demonstrated anomalies which could be explained on the basis of the concept (exceptionally phenomenological at that time) of the existence of a CEF potential of the same range as had been established for RE-based insulators by optical spectroscopy.

It is known that the result of the action of the CEF on the RE-ion is some release of *J*-multiplet degeneracy, depending on the parameters of the spin-orbit multiplet[2] and CEF potential, by a splitting into sub-levels distinguished by the projection of J_z. However, optical spectroscopy can not be effectively applied for metals, meaning that it seems no direct method to study the question of the reality of the suggestion about CEF effects in metals existed at that time.

The first results of neutron scattering experiments with a series of monochalcogenides (Bi, Sb, As, P) and monopnictides (Te, Se, S) of praseodymium were obtained at the high flux isotope reactor in Brookhaven and published by a group of American scientists on the cusp of the 1970s [4]. They presented convincing proofs of the existence of the CEF potential with a cubic symmetry in metallic compounds with a cubic crystal lattice. Neutron scattering spectra interpreted in accordance with Eqns (9) and (10) are shown in Fig. 3 as it appears with a time-of-flight spectrometer for PrSb powder.

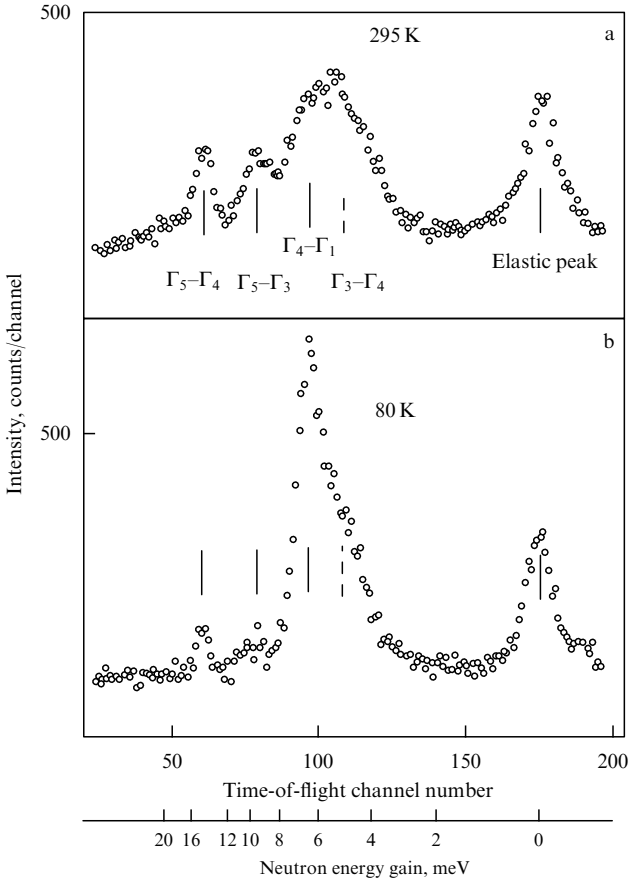

Figure 3. Time-of-flight spectra for double differential cross section of neutron scattering measured on a polycrystalline sample of PrSb at temperatures of 295 K (a) and 80 K (b). Marks show the positions of the elastic peak of nuclear scattering and dipole transitions between CEF levels according to the extracted level splitting scheme for the Pr^{3+} ion.

The total energy splitting of the RE-ion ground state multiplet (being degenerate for J_z in the free state) appears to be around 100 K,[3] which provides a natural explanation for low temperature anomalies of the physical properties of such compounds. At that time, in Europe the first experiments measuring the CEF excitations by neutron scattering were performed by scientists from Great Britain, Switzerland, and the USSR [6–10] independently of one another. As an example (Fig. 4), we present the results from the time-of-flight spectrometer at the IR-8 reactor at the Kurchatov Institute (Moscow) obtained in the early 1970s with the $PrAl_3$ system of hexagonal symmetry, where the number of levels and possible transitions is larger than for cubic systems, like PrSb. Results of the interpretation of these data allowed a definitive determination of the splitting scheme and allowed a description of the thermodynamic features in heat capacity and magnetic susceptibility to be obtained.

It is interesting to note that the result of [4] was a surprise for many scientists in the field and long seemed to be at odds with other similar studies. The authors of [4] defined the

[2] For RE ions, the total moment *J* [see Eqn (8)] appears to be a 'good' quantum number [5], meaning the energy of spin-orbit interaction producing the energy difference between the states with different *J* is much larger than probable CEF splitting. Therefore, for reasonable temperatures below $\sim 10^3$ K typically, only the lowest spin–orbit-multiplet with J defined by the Hund's rule can be populated.

[3] Note the numerical relationship 1 meV = 11.6 K = 8 cm^{-1} = 0.24 THz among units widely used in spectroscopy.

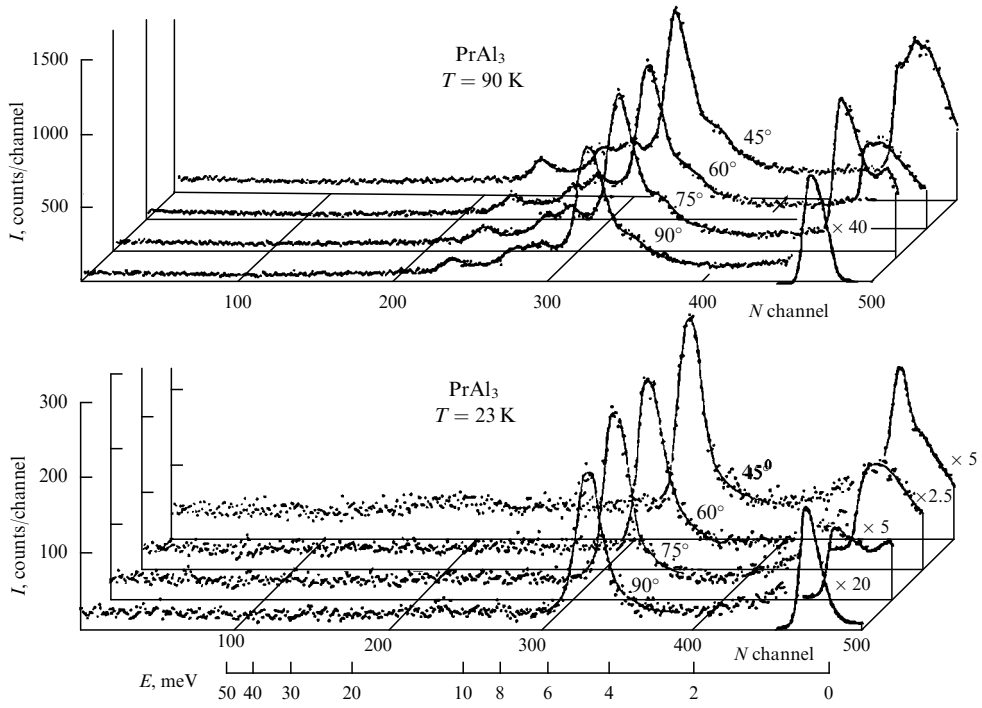

Figure 4. Time-of-flight spectra for a double differential cross section of neutron scattering measured in a polycrystalline sample $PrAl_3$ at temperatures of 23 K and 90 K at the Kurchatov Institute. A decrease in the scattering angle results in an increase in the peak intensities according to the magnetic form factor [Eqns (4)–(9)]. In the measurements, the energy transfer corresponds to the neutron energy gain process due to low incoming energy ($E_0 = 5$ meV). Therefore, the intensity of the inelastic peaks observed, as well as their number, decreases with the decrease in temperature. The elastic line is contaminated by coherent effects.

parameters of the CEF Hamiltonian from the splitting scheme for the whole series of seven systems. It appears that such parameters correspond to the simple point charge model with charges $= -2|e|$ located at the nearest neighbors of RE ions in a cubic lattice, from antimony to sulfur ions, and just with its formal valence of -2! This conclusion was very surprising and was discussed a long time in the literature, because, in this case, there was 'no room' for the effects of the conduction electron in the formation of the CEF potential.

But after the large number of subsequent measurements of metallic systems, even of the same family but based on neodymium [7], such a 'trivial' result (correspondence of the effective charges, being just phenomenological parameters, to the nominal valence) was never again obtained. That was a chance coincidence, but realized in one of the first experiments!

A similar 'curiosity' is connected with another 'pioneering' study [6] dealing with the same class of systems as in [4] but based on cerium (Ce). It appears in measurements that peaks from CEF transitions are considerably broadened in CeAs, and are not even observed for CeSb — the spectrum is dominated by a quasielastic signal. Later on, a similar result was obtained in our study [10] for hexagonal system $CeAl_3$. These observations were not adequately interpreted at that time, but later, after about 10 years, Ce-based intermetallic compounds started to be considered to be 'representatives' of a new class of Kondo systems (see Section 3.1). It must be noted that different mechanisms of line broadening in connection with CEF excitations in neutron spectra attracted a lot of attention in those years, but primarily the electron–phonon interaction was studied [11, 12].

A qualitative analysis of the great number of subsequent experiments allows us to reach several important conclusions: about the relationship of the CEF potential with local crystal symmetry in the vicinity of an RE ion which, in fact, serves as a 'sensor' of the CEF; about the existence of the considerable contribution to the CEF potential from conduction electrons; about the influence of the exchange interaction on the parameters of excitations observed in experimental spectra (energy, dispersion). It is necessary to point out that the role of conduction electrons appears to be related to their 'genetics' (atomic characteristics), as well as crystal structure. Thus, in the case of RE compounds with Al ($RE Al_2$ [13], $RE Al_3$[14, 15]), or with Pd ($RE Pd_3$ [13]), it turns out that 'reduced' CEF parameters do not change considerably when transferring from one RE ion to another. At the same time, for compounds with 3d-elements, for instance, with Ni or Cu, the replacement of one RE ion by another one, even the nearest one, results in a substantial change [16] in potential parameters (even to the sign).

There are many review articles devoted to the problem of describing and modeling the CEF in metals, starting from the first [17] up to following and relatively recent ones [18–21]. Experimental results of CEF neutron spectroscopy appear to be a reliable background for the interpretation and prediction of the anomalies in thermodynamics stipulated for the interaction of the f-electron shell with the CEF potential. Based on these results, theorists have made attempts to move outside the framework of the phenomenological approach to the CEF potential in metals. Nevertheless, disruptive results, providing the ability to form a unified *ab initio* model for CEF calculations, unfortunately, have not been found to date. In contrast to many other fields in modern condensed matter

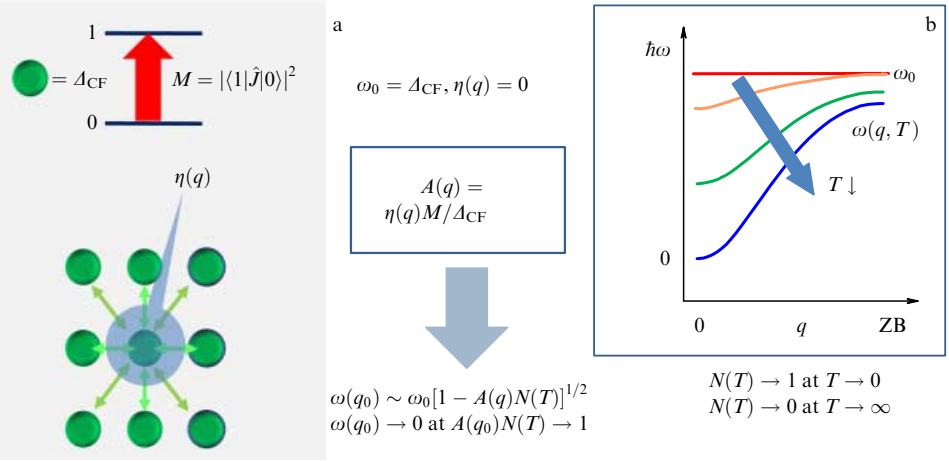

Figure 5. Formation of the f-electron state with polarization instability. (a) The interacting ions located at the lattice sites; each ion has two singlet states split by the crystal field. (b) The softening of the magnetic excitation mode for $A > 1$ in the reciprocal lattice point $q = 0$, where $\eta(q = 0) = \eta_{max}$; softening increases with decreasing temperature to the temperature of ferromagnetic ordering $T_c > 0$. ZB — Brillouin zone boundary where a dispersion curve closes.

physics, the task of defining the CEF potential is still the subject of experimental study.

Certainly, during formation of new direction of researches in neutron spectroscopy a methodology of neutron experiment has been developed considerably: the low temperature sample environment technique was introduced into routine operation; the methods for separation of the magnetic and latticed contributions to INS were developed and improved, in particular, wide-aperture detector systems for time-of-flight spectrometers have been designed. All of it extended experimental possibilities substantially.

Let us consider a number of rather brilliant, in our opinion, results of studies in the field of CEF effects along and in connection with some other actual problems of the physics of SCES, obtained by using neutron spectroscopy as attained by Russian experimentalists as well.

2.2 Induced magnetism

The phenomenon named 'induced magnetic ordering' was predicted theoretically in the work by B R Cooper and coworkers at the beginning of the 1970s [22]. The idea of the work was, in short, as follows. Let us assume that in some position in a crystal lattice an ion appears with singlet states (a ground state and an excited one) which are separated by the energy Δ_{CF} due to the action of a CEF potential. Thanks to this, the ion does not carry a magnetic moment. Between the above two states, the nonzero dipole matrix element M does exist. Let us assume that the ions take equivalent positions in the crystal lattice. It is clear that the system will keep the paramagnetic (Van Vleck) state up to zero temperature in the absence of inter-ion interaction.[4] But the introduction of inter-ion interaction described by a simple lattice sum over neighbors, for instance, like

$$\eta(\mathbf{q}) = \sum_{ik} \eta_{ik} \exp\left(-i\mathbf{q}\mathbf{r}_{ik}\right), \tag{12}$$

where η_{ik} is the pair exchange integral between RE ions located at positions i and k, changes the physical situation qualitatively: the dipole matrix element, along with the inter-ion interaction, resulting in the mixing of wave functions, 'works' against the crystal field which 'separates' it. In this way, the joint action of these interactions results in the appearance of the polarization factor. The latter turns out to be the origin of the induced magnetic moment on each ion in the lattice and the simultaneous orientational ordering of this collection of moments. Cooper showed that the criterion of the establishment of the induced magnetic ordering for this system is the fulfillment of the following condition for the A-parameter:

$$AN(T) = \frac{M\eta(\mathbf{q})}{\Delta_{CF}} N(T) \geqslant 1, \tag{13}$$

where $N(T)$ is the temperature factor determined by the population difference between two intial states ($N(0) = 1$).

Now, let us see how the excitation spectrum of the ionic system would transform upon an increase in the A-parameter from zero. From a general consideration, it is obvious that the spectrum should transform from a single site spectrum to a dispersion one with energy dependence over wave vector q simply due to the fact that polarization instability develops in the periodic lattice. Cooper discovered that fulfillment of criterion $A = 1$ corresponds to the excitation energy $\omega(\mathbf{q})$ arriving at the zero value at the specific point $\mathbf{q} = \mathbf{q}_0$ of reciprocal space, which is defined by the position of the maximum of $\eta(\mathbf{q}) = \eta(\mathbf{q}_0)$.

This means, in fact, that the magnetic crystal lattice site is formed at $\mathbf{q} = \mathbf{q}_0$ in the Brillouin zone and the corresponding Bragg peak should appear in the magnetic diffraction pattern. In this way, the magnetic phase transition to the long range ordered state appears to be connected with the formation of a magnetic 'soft mode' originating from an initially single-site CEF excitation, as illustrated in Fig. 5. In general, the dispersion relation for such excitation at temperatures $T > T_0$ at which the transition temperature T_0 [defined by Eqn (13) when $A = 1$] is described in the form

$$\frac{\omega(q, T)}{\omega_0} = \left(1 - \frac{M\eta(\mathbf{q})}{\hbar\omega_0} N(T)\right)^{1/2}, \tag{14}$$

where $\hbar\omega_0 = \Delta_{CF}$.

There have been several attempts to check the idea of [22] using real systems with a singlet ground state in the CEF [23, 24] but, due to various reasons, a clear demonstration of the

[4] Nuclear magnetism effects are not taken into account.

effect predicted has been realized relatively recently in [25]. In this study, we came most close to compliance with the important condition of the model — to deal with two singlets isolated in the physical sense. The system under study was binary compound PrNi with a temperature of ferromagnetic ordering of $T_c = 21$ K.

A single crystal sample of PrNi has been used for neutron spectroscopy experiments. In measurements of the decrease in temperature approaching 21 K, a continuous drop, practically to zero, in the frequency of one of the magnetic modes at $q = 0$ (that is, the Brillouin zone center) has been observed, as shown in Fig. 6a. Initially, this mode is related to one (lower) ($\hbar\omega_{01}$) of two crystal field excitations ($\hbar\omega_{01} \sim 2.5$ meV and $\hbar\omega_{02} \sim 3.6$ meV) between the ground state and two other singlets discovered in the spectrum of the paramagnetic single crystal $Pr_{0.07}La_{0.93}Ni$. It is important to note that these transitions from the ground state singlet carry no less than 85% of the total magnetic scattering cross section, allowing us to disregard both the interaction of excited states among one another and the existence of other CEF levels.

Due to the low (orthorhombic) crystal symmetry, the degeneracy of the 9-fold ground state multiplet of the Pr^{3+} ion is released up to singlets. Thus, the system is in full correspondence with requirements of the Cooper model with two specifications: (1) the level scheme is not double but triple, and (2) for this substance, the crystal lattice structure is not described by the Brave lattice. Owing to the latter point, we get the opportunity to observe the formation of acoustic and optic modes from each of two initially single site CEF modes. Thus, in PrNi single crystal measurements on a three-axis spectrometer, we have observed 4 different modes with specific dynamical structure factors. Model calculations based on formulas from [22] modified due to the real crystal structure of PrNi (that is, crystal anisotropy, values of the dipole matrix elements, and real dynamical structure factors) provided a quantitative description of all the experimental data collected for different directions and different Brillouin zones of the crystal [26]. Examples are shown in Fig. 6b: experiment and calculation for dispersions along $(0, 3 \pm k, 0)$, direction measured from the point $(0, 3, 0)$, results for direction $(1 \pm k, 0, 0)$ are presented in Fig. 6a.

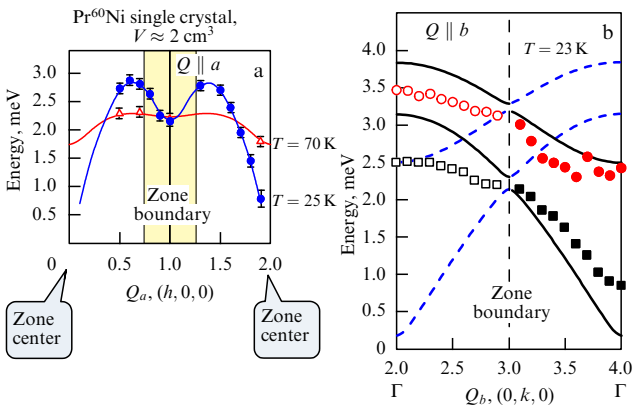

Figure 6. Experimental data (symbols) and results of calculations (lines) based on the double-sublattice model with four exchange constants (interaction of 1st and 2nd neighbors in both sublattices) for dispersion of magnetic excitation in a single crystal of $Pr^{60}Ni$ (isotopically pure for the Ni element). (a) Soft mode formation upon temperature decrease. (b) Modes measured at 23 K for different directions. Dashed lines show modes with calculated zero intensity for this particular direction from a particular lattice site.

Taking into account the relative simplicity of the model used (only 4 exchange constants for the double-sublattice representation), the correspondence between calculated results and experimental data is amazingly good.

2.3 Crystal field in high temperature superconductors

The launch of neutron studies of HTSC-cuprates corresponds to the period at the end of the 1980s to the beginning of the 1990s, which was defined by the availability of good quality and large enough single crystal samples of these anisotropic materials. The huge and widely spread diversity of the experimental data has been collected and presented in different reviews and books from that time. Therefore, here we will focus only on publications related to the problem of CEF effects in connection with the study of HTSC phenomena.

From the first approach to neutron scattering magnetic spectra obtained for HTSC compounds like $2-1-4$ (La_2CuO_4) as well as $1-2-3$ ($YBa_2Cu_3O_7$), it was established that CEF effects are strong enough in these systems, where overall splitting exceeds 100 meV. Exchange interaction effects result in the development of the dispersion of corresponding excitations at low temperatures; the temperature dependence of the intrinsic width of single-site CEF excitation appears to be connected with the variation of the density of electron states at the Fermi energy, in particular due to superconducting gap formation (these effects were studied later in fine detail [27]).

In the study of HTSC materials, it was concluded that the local inhomogeneity of the charge distribution may take place due to strong electron-electron and electron–phonon interaction. The high sensitivity of CEF effects to the local charge distribution was discovered in pioneering neutron spectroscopy studies of RE-intermetallics (see, for example, [28]). Therefore, the neutron spectra of the excitations between CEF-split levels can be used as a good 'indicator' of the presence of charge inhomogeneity in the materials under study. In $REBa_2Cu_3O_{7-\delta}$ compounds, the RE ions take positions between two CuO_2 planes, which allows using the CEF spectroscopy as an instrument for the study of the processes of doping (with oxygen first of all) and related charge redistributions in these planes on the microscopic (cluster) level.

The neutron spectroscopy technique made possible the direct observation and quantitative description of the mechanisms of charge transfer from CuO chains to CuO_2 planes; thus, information about cluster formation related to the appearance of 'frustrated phase separation' became available.

This idea has been used as background for the study of the problem of local charge inhomogeneity developed due to different kinds of doping in HTSC in a series of studies by an international group of Russian and Swiss scientists. The particular results were obtained for $1-2-3$ type systems with oxygen concentration variation [29, 30] and replacement in the RE-ion position [31, 32].

The phase separation effect, in fact, corresponds to the existence of a considerable difference between local electron charge density in the vicinity of doping ions and charge density averaged over the crystal. This difference becomes apparent via the development of a superposition structure of CEF spectra. Its different components may be put into correspondence with a number of local surrounding configurations for RE-ions existing in the sample. Its relative

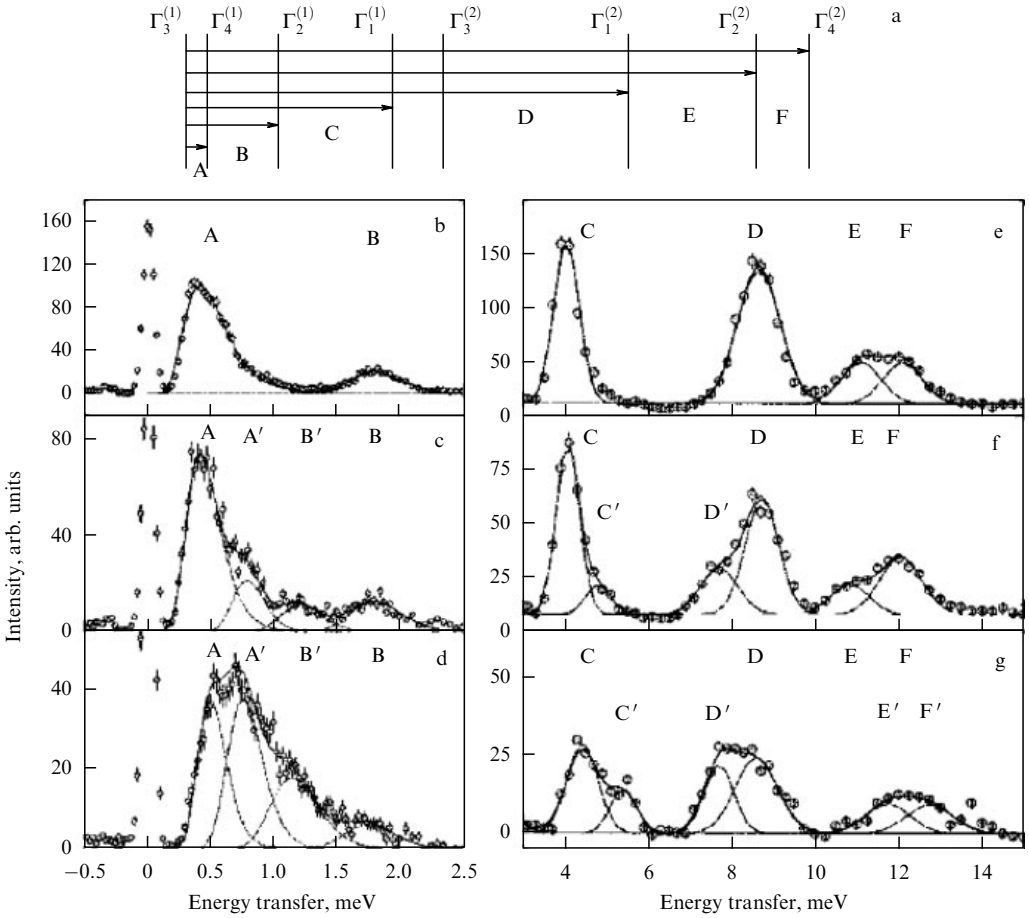

Figure 7. (a) Splitting scheme obtained for a number of low energy CEF levels for $(HoCa)Ba_2Cu_3O_7$; the experimentally observed transitions are marked by arrows with symbols A, B, ..., F. (b–g) Neutron scattering spectra of $Ho_{1-y}Ca_yBa_2Cu_3O_7$ measured at = 1.5 K for $y = 0$ (b, e), 0.1 (c, f), 0.25 (d, g), respectively) on a three-axis spectrometer. Left side (b–d): spectra measured with high experimental resolution for the lowest energy peak of CEF excitation ($Q = 0.85$ Å^{-1}, fixed final neutron energy is $E_f = 3.5$ meV). Right side (e–g): spectra with $Q = 1.8$ Å^{-1} and $E_f = 7$ meV. Lines show the approximation of the peaks by spectral functions. Symbols A′, B′, ..., F′ represents the splitting scheme modified by the RE ion surrounding transformation (from [32]).

spectral contribution is defined by the probability distribution of the realization of a particular type of RE-ion surrounding (Fig. 7).

These effects have been studied with the Er 1−2−3 system in the range of oxygen concentrations $\delta = 0-1$, and with Ho 1−2−3, where Ho is replaced by Ca. Neutron scattering spectra from this study are shown in Fig. 7. It demonstrates quite clearly the bulk inhomogeneity of CEF effects existing in the samples studied. Detailed and multilateral neutron spectroscopy studies of CEF effects in systems with different doping levels have been carried out [31, 32]. The authors have developed the concept of charge transfer related to doping, the formation of two-dimensional charge distribution in the planes (model of a periodic system of charged stripes). This made an essential contribution to the understanding of the modification of the properties of HTSC-cuprates on transferring from underdoped to overdoped regimes and shed light on the problem of pseudogap formation.

3. Systems with effects of hybridization between f-electrons and itinerant electrons. 'Anomalous' rare earth intermetallic compounds

The rapid grow of the neutron scattering study of SCES at the initial stage in the 1980s and 1990s (a number of detailed reviews exist for that period [17–21]) resulted in the development of a quite simple and clear classification scheme for a variety of synthesized binaries and more complicated systems based on f-elements. The base of this scheme is the combination and competition of crystal field effects (characteristic splitting scale Δ_{CEF}), exchange driven magnetic ordering (interaction energy parameter J_{ex}), and hybridization interaction (energy scale V_{cf}).

Depending on the extent of hybridization with respect to the other parameters, first of all, to CEF-splitting, the ground state appears to be 'normal' — that is, with local a magnetic moment ($\Delta_{CEF}, J_{ex} > V_{cf}$) or a Kondo-type ground state is formed (in an ordered lattice of Kondo-ions, it is named a 'heavy fermion'); when $\Delta_{CEF} \sim V_{cf}$, or when the hybridization dominates ($\Delta_{CEF}, J_{ex} < V_{cf}$), the intermediate valence state is realized, the latter corresponding to the partly delocalized f-electron. In the last case, strong spin fluctuations are observed which manifest themselves by a dominating quasielastic contribution to the magnetic neutron scattering spectra. In the heavy fermion regime, the existence of broad quasielastic signal (the line-width is comparable to the energy of excitation) inelastic peaks related to CEF transitions, along with a quasielastic signal with quite specific temperature dependence of its spectral function, is observed. The width of the quasielastic signal serves as an important

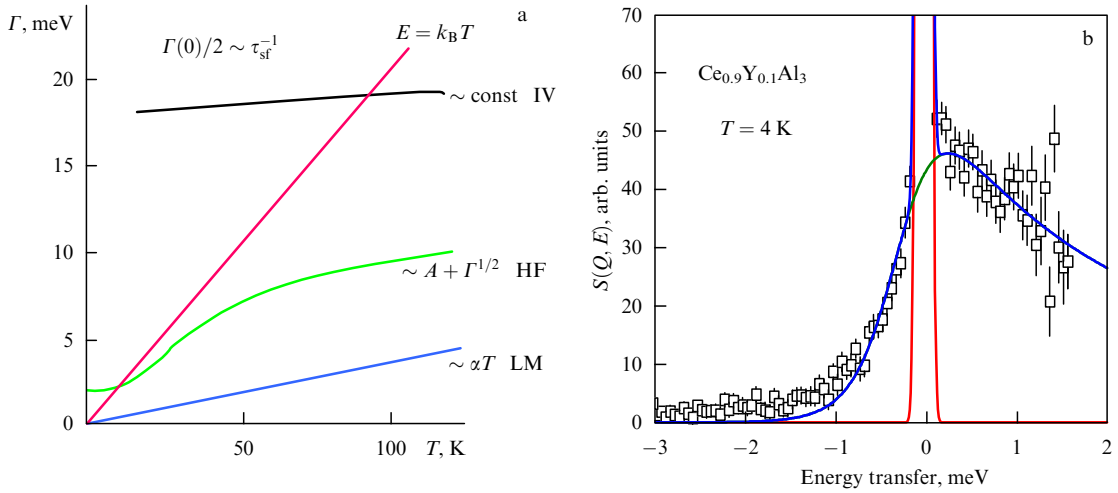

Figure 8. (a) Quasielastic component of magnetic excitation spectra as 'classification' characteristics of SCES systems for different types of regimes: LM (local magnetic moment), HF (heavy fermions), IV (intermediate valence); τ_{sf} is the period of spin fluctuations, Γ is the width of the quasielastic line at half maximum). (b) Typical spectrum of a spectral function is shown for the heavy fermion system $CeAl_3$ at low temperature when characteristic asymmetry of the scattering function is observed due to the temperature factor [see Eqn (1)].

characteristic of the f-electron state — the energy of spin fluctuation, which appears to be closely related to the concept of Kondo temperature ($T_K \sim \Gamma_{qe}/2 = k_B T_{sf}$). A diagram of the relationship between temperature and quasielastic line-width for different physical regimes of SCES is presented in Fig. 8.

In this way, one can distinguish, based on the character of the spectra, which type of regimes is realized for the subject of study. This serves as good support, in addition to the thermodynamic methods of classification and, in some cases, as a unique objective criterion.

In Sections 3.1–3.4, the number of results obtained with our participation are presented and discussed, which are interesting from the point of view of manifestation of some new effects in strongly correlated systems with not negligible hybridization. Some of these are comprehensive studies of magnetic and lattice dynamics and their mutual influence and interconnection.

3.1 Heavy fermion systems: the example of $CeAl_3$

$CeAl_3$ is a system from which, in fact, the physics of concentrated Kondo systems, later getting the name 'heavy fermions' [33], started [34]. By a convergence of circumstance, this compound was one of the first of our subjects in neutron spectroscopy studies [10] in the years when adequate physical ideas had just started to be formulated. At that time, we could not provide a clear physical interpretation of the unusual spectral characteristics of its experimentally obtained magnetic spectral function. First of all, it is unusually large, comparable to the energy of the excitations, the width of the inelastic peaks almost without observable temperature dependence. Moreover, there is a broad and intensive quasielastic scattering contribution to the spectra with the square root type of temperature dependence of width and some residual value (in the range of $10^0 - 10^1$ K) at $T \to 0$ (see Fig. 8), as was shown later in [35]. At the early times of [10], we were limited by the task of defining just the splitting scheme (three doublets: for the ground state one, a dipole transition between its components is forbidden) from spectral function parameters. It is necessary to mention that even this particular point was for a long time a subject of study and discussion [36–39].

After a long time, interest turned back to this compound and more detailed studies started; results are presented in publications [38, 40, 41]. At the core were problems of understanding the effects of 'dynamical screening' of the local magnetic moment which develops on decreasing the temperature. It is related to the effects of scattering with spin-reversal of the conduction electrons on the localized moments, which results in the formation of a resonant peak in the electron density of state near the Fermi energy. This peak corresponds to the formation of the heavy fermion state and, it is believed (see, for instance, [42]), serves as a source of the thermodynamic and kinetic manifestations of the HF state in the physical properties. In particular, we wanted to establish whether charge redistribution, along with the obvious spin density redistribution responsible for 'screening' the local magnetic moment, takes place in the local vicinity of the Kondo ion. It was also interesting to study what the transformation of the excitation spectra of the RE ion is (change in energy, intensity, widths of inelastic and quasielastic peaks), simultaneously with the formation of HF resonance. How does this transformation (if any) depend on the extent of the hybridization?

Experimental answers to these questions have been obtained in a number of studies [38, 40, 43], where for the first time in neutron spectroscopy of SCES the 'impurity mark' (or 'sensor') method was used, which allows obtaining information about the properties of electrostatic potential in the crystal matrix, in the present case, the heavy fermion one. Experimentally, for $CeAl_3$, some part of the Ce ions in the sample are replaced by the nearest RE ion in the series, Pr^{3+}, the CEF-characteristics of which are well established and checked by the measurement of the same amount of Pr^{3+} in the nonmagnetic isostructural matrix $LaAl_3$. It appears in [40, 43] that no difference between the heavy fermion (based on Ce) and nonmagnetic analogue (based on La) with respect to CEF parameters for Pr^{3+} is observed at the very low temperatures (≈ 1.5 K) in these measurements. Nevertheless, the difference has been observed in relaxation

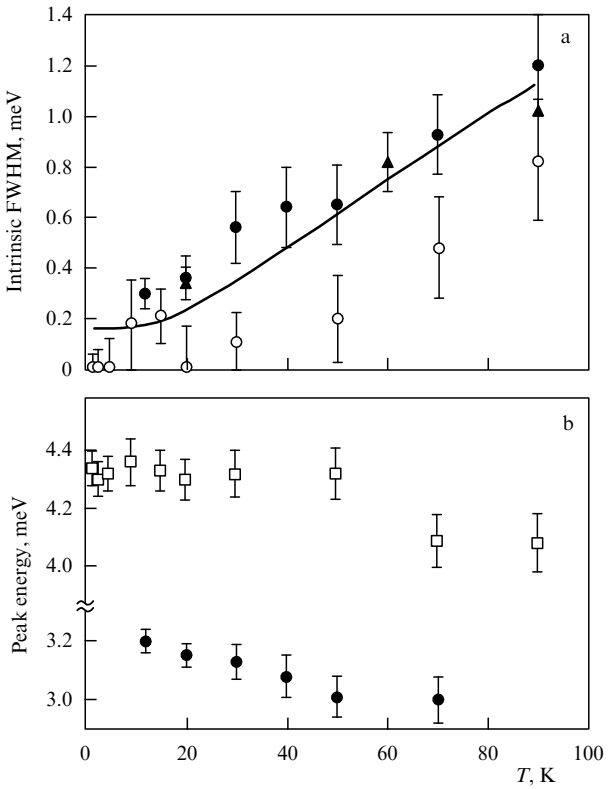

Figure 9. Experimental temperature dependences of the parameters of the peak in the neutron spectra corresponding to the transition $\Gamma_1 \rightarrow \Gamma_6$ for the Pr^{3+} impurity ion in the CEF of $CeAl_3$ and $LaAl_3$ compound (measured at $Q = 1.4$ Å^{-1}): (a) intrinsic widths (after correction to the resolution function); the line presents a calculation by the standard relaxation model; (b) energy of the peak. White symbols correspond to $Pr_{0.03}Ce_{0.97}Al_3$, black to $Pr_{0.03}La_{0.97}Al_3$.

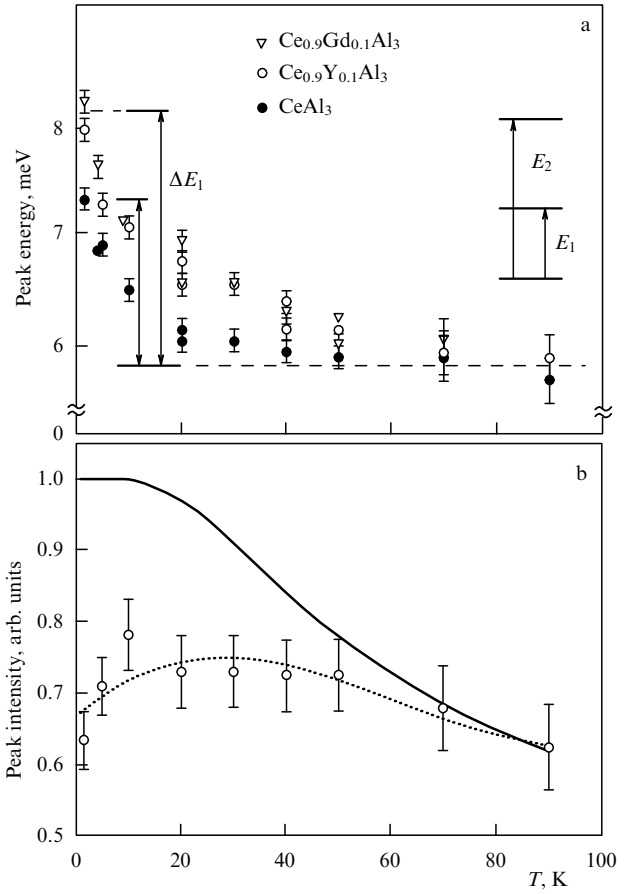

Figure 10. Experimental temperature dependence of energy (a) and intensity (b) of the main peak (E_1) in CEF excitation spectra for different substitutions in the RE sublattice of $CeAl_3$. In (a): black dots — $CeAl_3$, white dots — $Ce_{0.9}Y_{0.1}Al_3$ ('chemical' pressure), triangles — $Ce_{0.9}Gd_{0.1}Al_3$ ('chemical' pressure + magnetic impurity); on the right side of (a) — splitting scheme for Ce^{3+} in CEF of $REAl_3$. In (b) circles — experiment for $CeAl_3$ (dotted line is a visual approximation), line — standard [see Eqn (6)] calculation for the CEF splitting scheme.

characteristics of the impurity Pr ion.[5] It is interesting that the relaxation rate of its CEF excitations is obviously suppressed (not increased, as could be expected!) with a decrease in temperature, in contrast to its nonmagnetic analogue [38] (Fig. 9). This circumstance was interpreted in [44] as the manifestation of the more complicated than usual Heisenberg-type mechanism of spin-spin relaxation in this type of system. This new channel is related to a probability of more than on 1 of spin transitions with S_z change, due to the impurity of the f-electron states induced by hybridization.

Another effect studied in [38] is connected to the spectra of the Ce Kondo ion in $CeAl_3$. It appears as a renormalization of the energy and intensity of inelastic peaks (Fig. 10) 'genetically' related to the transition between CFE levels of Ce^{3+}, as a function of decreasing temperature to $T \ll T_K$ (minimal measured temperature in [38] is 0.03 K). This renormalization appears not to result from the electrostatic potential changes but is caused by changing the scale of hybridization, as was discovered after detailed analysis. The specifics of the renormalization caused an increase in the energy of excitations (up to 20%) and 'pumping' of the intensity from the inelastic peaks into the quasielastic peak (also about 20%) by a decrease in temperature below the value comparable to CEF splitting: 50 K $\sim \Delta_{CEF} \gg T_K$. The driving forces of the above phenomenon are not clear yet. It is necessary to mention that the abrupt change in the character of the relaxation of the excitation for an impurity Pr^{3+} paramagnetic ion discussed above (see Fig. 9) is observed in the same temperature range. These effects could be related to the influence of the hybridization, which is qualitatively in correspondence with the interpretation of experimental data presented in Fig. 10. It evidently shows a sensitivity to the influence of 'chemical' pressure (a stronger shift of the peak energies for $Ce_{0.9}Y_{0.1}Al_3$) and the absence of any extra effects of strong magnetic moments ($Ce_{0.9}Gd_{0.1}Al_3$). There is some evidence that similar renormalization effects exist in other heavy fermion systems ($CeCu_2Si_2$, $CeCu_5$).

Following the conception of theoretical study [45] where the formation of the ground state of the Kondo system is considered, one can assume that just the evolution of the population of CEF states is the origin of the transformations in the excitation spectrum upon a temperature decrease. This corresponds to the fact that the effective degeneracy of the f-electron state (it is defined by the population) plays a principal role in the formation of the resonance Kondo level, driven by hybridization.

[5] The naïve approach to the estimation of the influence of the huge electron density of states at the Fermi level on the width of CEF excitations of the 'normal' paramagnetic ion should result in the total damping of the considered peak, that is, its total wipe out by substantial broadening progressing with decreasing temperature.

3.2 Intermediate valence

Typical 'classical' representatives of valence-fluctuative or intermediate valence systems are SmB_6, Sm(Y)S systems. In fact, precisely the study of SmB_6 properties initiated by Soviet scientists in the 1960s [46] turned out to be the starting point of investigations aimed at understanding this physical phenomenon. The physics of intermediate valence has for a long time been associated with the picture of charge fluctuations between the f-shell and conduction band, being represented by the symbolic equation suggested by L Hirst [47]:

$$f^n \leftrightarrow f^{n-1} + e^-_{\text{in conduction band}} . \quad (15)$$

Obviously, it was determined by the discovery of the phenomenon of 'lattice collapse',[6] revealing negative values of the elastic C_{12} modules, the anomalous softening of some longitudinal acoustic phonons. A fundamental physical study of this phenomenon required spectroscopic measurements of single crystals, combining the study of the magnetic and lattice excitations. These approaches have been carried out with the use of neutron spectroscopy [48–51].

As has been mentioned in the Introduction, neutron spectroscopy appears to be quite 'compatible' with valence fluctuations by the characteristic interaction time of neutrons with phonons and magnetic moments [51]. The use of neutrons allows us to establish a number of previously unknown features of the IV state which become apparent in atomic and magnetic dynamics [52], and on this basis new ideas dealing with the quantum mechanical origin of this state [53, 54] have been developed.

Comprehensive studies of lattice and magnetic excitation spectra in a wide range of temperatures and intermediate valence values for systems based on SmB6 and SmS poly- and single crystal samples produced from pure isotopic ^{154}Sm and ^{11}B materials have been carried out. The influence of the IV state has been studied on lattice dynamics on the level of phonon dispersion [55–58], magnetic excitation spectra, including the intermultiplet transitions of both competing configurations f^6 (Sm^{2+}) and f^5 (Sm^{3+}) [59–69] for two cases: homogeneous mixed valence (i.e., intermediate valence) and the inhomogeneous state which is realized for Sm_3Te_4 [70].

Similar detailed studies have been realized for the IV compound CeNi [71–78]. We have observed clear anomalies in phonon spectra for the first time for Ce-based systems, and the formation of a spin gap in magnetic excitation spectra have been studied for CeNi-based compounds. Let us consider the most brilliant and important results from the above mentioned series and the corresponding physical findings.

3.2.1 Electron–phonon interaction: resonance violation of adiabatic approximation. Issues concerning the influence of valence instability on the lattice dynamics have been analyzed recently in review [79], and here it will be considered briefly to avoid unnecessary repetition.

From early work on the lattice dynamics of SmS in the IV state (it is realized experimentally by an external pressure of 5 kbar or by replacing Sm with Y — that is, the so-called effect of 'chemical' pressure) [69, 80, 81], two main features were known: anomalous softening of the longitudinal acoustic phonon mode and the appearance of the dispersionless extra- mode at about 20 meV of energy in the gap between the acoustic and optic modes in the phonon spectrum. The latter were discovered in measurements of (Sm, Y)S [81] and were initially related to the quasilocal vibrations[7] of Y-atoms; this interpretation was not confirmed later.

Experiments with SmB_6 single crystals [55–58] have shown that the lattice dynamics are characterized by anomalous softening of the longitudinal acoustic modes, as well as the existence of some extra vibration modes. One of these is a dispersionless mode in the gap between the acoustic and optic branches (in analogy with the one observed for (Sm, Y)S); another one — a mode in the vicinity of the acoustic frequencies near the Brillouin zone boundary — is characterized by the strong temperature dependence of its energy. It was clear that quite similar effects are observed for two systems different in atomic structure and the character of interatomic force interactions; therefore, this is nothing more than manifestations of the electron–phonon interaction specific for the IV state.

The first of the above effects — softening of the acoustic modes — could be described in the framework of traditional models and approaches to lattice dynamics, for instance, by taking into account the influence of 'breathing' deformations (normal vibrations with full symmetry) of the nearest surroundings of RE ions related to charge fluctuations [55] on 'usual' phonon spectra.

Nevertheless, the second type of effect — there are 'excess' modes from the point of view of the usual (adiabatic) theory of lattice vibrations [57] — requires new approaches to the description of these modes and understanding of the IV state as well. The explanation of the above phenomenon suggested in [53] is based on the assumption that the adiabatic approximation traditional for the physics of lattice dynamics is violated due to the existence in IV system of soft electronic modes resulting from charge transfer effects (so-called 'charge fluctuations'). As a result, the ratio between energies of phonon $\hbar\omega_{ph}$ and electron $\hbar\omega_{el}$ sub-systems is changed from the usual one, $\hbar\omega_{el} \gg \hbar\omega_{ph}$, to $\hbar\omega_{el} \sim \hbar\omega_{ph}$ for some specific phonon modes.

This, in turn, results in the emergence of new, so-called [53, 57, 58] vibronic modes in the phonon spectra that are additional with respect to phonon modes caused by the crystal structure. This phenomenon has been called *resonance violation of adiabaticity*.

3.2.2 Resonance mode and intermultiplet transitions in the magnetic neutron scattering spectra of SmB_6 and Sm(Y)S. The study of the magnetic excitation spectra in poly- and single crystal samples provides a number of facts important for IV phenomenon physics. Corresponding measurements with polycrystals were carried out for the first time in a wide range of energy transfer (up to 180 meV) by the method of time-of-flight spectroscopy at a pulsed neutron source. Single crystal samples were studied using a high-flux three-axis spectrometer positioned in the thermal neutron beam of a nuclear research reactor.

[6] This concept is related to the isostructural electron phase transition, which is accompanied by an abrupt change (up to 15%) in the volume of the unit cell. Metallic Ce or insulating SmS are examples of systems demonstrating such a phase transition under external pressure.

[7] In experiments on binary compound SmS under pressure, the corresponding energy range was not measured.

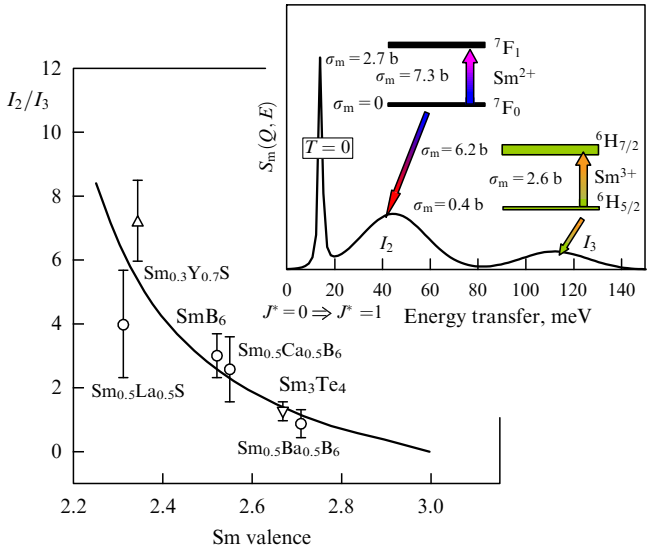

Figure 11. Intermultiplet excitations in the spectra of SmB_6. The ratio of the intensities of the intermultiplet transitions (broad peaks in the inset) as a function of the average valence of Sm; the points are neutron experimental data; the line is calculations using average valence defined from separated experiments. Shown in the inset is the schematic presentation of the experimentally observed spectra of magnetic neutron scattering. The relationship between dipole intermultiplet transitions with corresponding magnetic scattering cross sections (σ_m) and observed spectral peaks is shown by arrows. The narrow peak (14 meV) appears in the spectrum only at temperatures below 50 K. (From publication [66].)

The first fact which was obtained by the time-of-flight experiments [59, 64–66] was the existence of the characteristic peaks in the f-shell ground state excitation spectra, mainly expected from the traditional concept of IV (that is, the existence of two f-electron configurations with interconfigurational fluctuations between them as the background of IV phenomena). These peaks are quite broad ($\Gamma/2 \approx 10-15$ meV) and originate from the intermultiplet transitions specific to the two 'competing' configurations of Sm: f^6 and f^5, at energies of 36 meV and 125 meV ($J = 0 \to J = 1$ and $J = 5/2 \to J = 7/2$, respectively). A very important but unexpected result obtained by inelastic magnetic neutron scattering was that at low temperatures a very narrow peak with an energy of around 14 meV is observed (its existence was first observed in experiments [82] with SmB_6). Its width for SmB_6 has been limited by the resolution of the spectrometer and in this sense was at least an order of magnitude[8] less than for intermultiplet transitions. Magnetic constituent of the experimental spectral function of SmB_6 is shown schematically in the insert of the Fig. 11.

An essential result of the work is the study of the relationship of the parameters of the spectra with the valence state of samarium, which was fulfilled in samples with a variation of the average valence [65, 66] realized by the variation of composition (substitution of La, Ca, Ba for Sm in SmB_6 or substitution of Y for Sm in SmS). The influence of the valence variation on the low energy peak is quite different from the reaction of broad intermultiplet transitions. The latter simply change their relative intensity, following the average valence (see Fig. 11), which means that its behavior was approximately similar to that of the peaks in X-ray absorption spectra (XANES) with only one substantial difference — the width of the neutron peaks unambiguously indicates the fast relaxation of spin-orbital states ($\approx 10^{-12}-10^{-13}$ s). The narrow peak, on the contrary, changes just its energy (Fig. 12): when valence moves from 2.55 (SmB_6) to 2.2 ($(SmLa)B_6$) (an increase in the contribution from the f^6-configuration), its energy gradually increases, ensuring the extrapolated value of about 36 meV for the valence of 2+, and, vice versa, upon changing the valence from 2.55 to 2.8, its energy moves to zero. Moreover, unlike the intensities of wide intermultiplet peaks as functions of momentum transfer (Q) simply following corresponding dipole form factors, the form factor defined for the narrow low energy peak [62, 65, 66] appears to be highly dependent on the valence. Upon increasing the average valence from 2+ to 3+, the form factor becomes steeper than the intermultiplet dipole one (see Fig. 12). This effect, in the most straightforward way, can be related to the increase in the extent of the spatial delocalization of electron/spin density. Detailed measurements carried out with a single crystal of SmB_6 on a three-axis spectrometer have shown [61, 62] that a form factor

[8] Precise measurements recently carried out by neutron spectroscopy show that its width does not exceed 100 μeV.

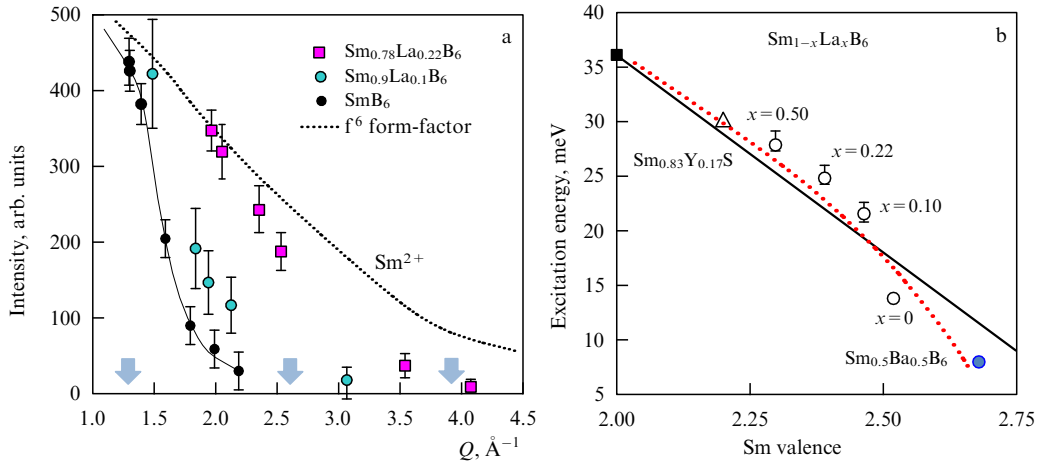

Figure 12. Characteristics of low energy excitation ('resonance mode') in $Sm(M)B_6$ systems. (a) Mode intensity as function of momentum transfer (Q) along the direction (q, q, q). The vertical arrows define the positions of the Brillouin zone boundaries. (b) The energy of this mode as a function of the valence. All measurements are done at $T \approx 10$ K. (From [66].)

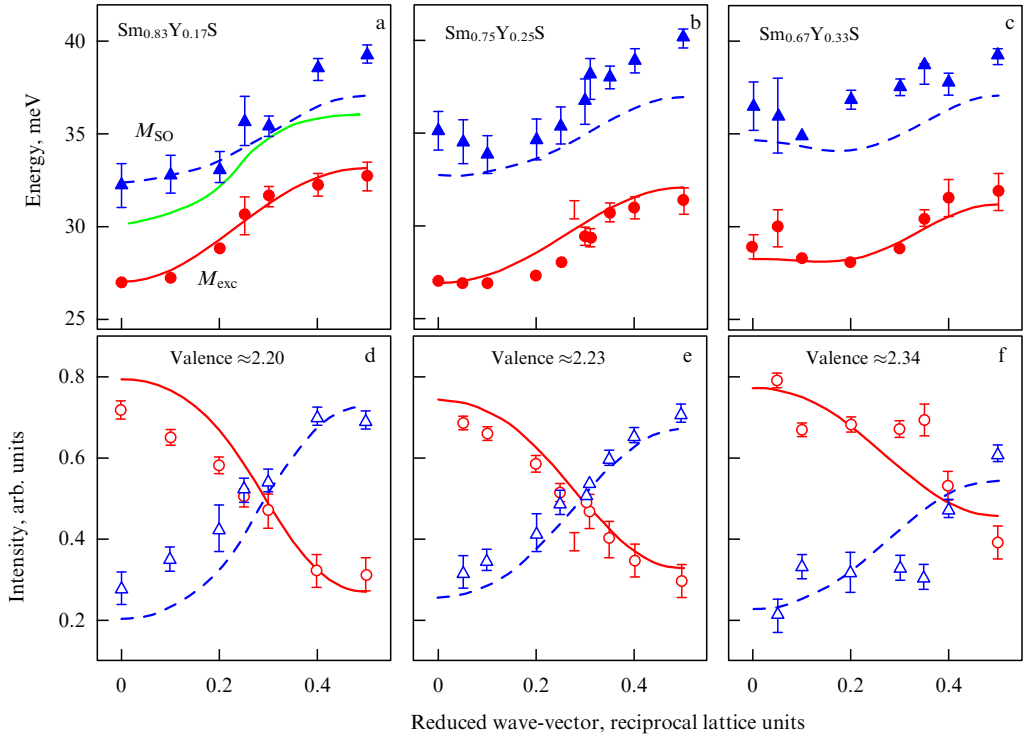

Figure 13. Energy — (a–c) and intensity — (d–f) for magnetic modes in the [111] direction in $Sm_{1-x}Y_xS$ for $x = 0.17$ (a, d), 0.25 (b, e), 0.33 (c, f) single crystals. Circles — resonance mode (M_{exc}), triangles — intermultiplet transition (M_{SO}). Solid and dashed lines — model calculations from [69] which take into account the exchange interaction and mode-mode hybridization. Green line in the (a) — dispersion for the intermultiplet transition for pure SmS according to data [83]. Measurements were done at $T \sim 10$ K.

of a 14-meV excitation not only dramatically decreases with an increase in the Q value (see Fig. 12) but is strongly anisotropic in the Brillouin zone and its intensity maximum exists along the [111] direction. However, this is true only for pure SmB_6; upon doping it with La (which results in the valence decreasing to Sm^{2+}), the character of the angle dependence changes greatly, appearing more isotropic, while the energy of the excitation grows.

The above discussed features of the peak at 14 meV in SmB_6 are studied at low temperatures in the range of 2–10 K. As the temperature increases, starting from 40 K, it begins to lose intensity and becomes broader, practically disappearing at temperatures approaching 80 K. At this and higher temperatures, the quasielastic scattering signal, which was not observed at low temperatures [62], starts to dominate in the low energy transfer spectra ($\Gamma/2 \sim 7-10$ meV); the Q-dependence of the quasielastic intensity appears to be quite weak and smooth (its determination is a separate and serious task).

The full number of features of this low energy excitation (relation between the energy and state of the f-electron system, localization in the q-space, temperature dependence and evolution of the low energy part of the spectra combined with a spin gap closing) closely resemble properties of excitation defined as a 'resonance mode' and observed in actively studied copper oxide and iron-based high temperature superconductors, and some other heavy fermion and Kondo compounds. Taking into account this analogy, the above excitation can be treated as some kind of 'resonance mode' which exists in a spin-gap of magnetic excitation spectra of Sm-based IV systems. This approach appears to be confirmed by studies of Sm(Y)S and some other systems, in particular, Eu-based intemetallics (see Section 3.4.3).

What is the real difference between $Sm_{1-x}Y_xS$ and SmB_6, if we move away from the particular features of crystal structure (the first is ionic crystal, the second is closer to covalent bonding in the three-dimensional cluster framework) and the type of doping material Y (not La, Ca, or Ba) necessary to provide any extent of intermediate valence?

The difference is that some extent of exchange interaction between RE ions is inherent in SmS (here, the distance between them is much shorter than in SmB_6), the existence of such interaction being confirmed experimentally by the observation of intermultiplet transition $J = 0 \rightarrow J = 1$ [83] in a single crystal. For pure SmS where Sm is in the f^6-state, in analogy with the above considered (see Section 2.2) induced magnetism, an exchange interaction is realized in some dispersion of singlet triplet excitation [$\hbar\omega_0 = 36$ meV, see Eqn (14)]. Studying the Sm(Y)S sample in the IV state, it is possible to get an answer to the question of how the inter-ion exchange realized under IV conditions, meaning in combination with spin fluctuations.

Results of an experimental neutron spectroscopy study of samples of $Sm_{1-x}Y_xS$ with different contents of Y in the range $0.17 < x < 0.33$ are presented in [68, 69]. It appears that the initial intermultiplet excitation and new resonance mode, typical for the IV state, keep the dispersion character for both excitations, in spite of the considerable (0.2–0.4) deviation of the valence from integer value (2+). The dispersion observed (Fig. 13) appears to be described by the very similar set of constants as used for the initial SmS. What is new is that between observed excitations (intemultiplet and resonance mode) the mode-mode interaction takes place, which influences the dependences of the energies and, essentially, of intensities from the reduced wave vector in the Brillouin zone. This gives direct evidence of their symmetry

identity, which appears to be an essential argument in the verification of the excitonic model of the IV state suggested by Russian theorists [53, 54] for Sm-based systems.

The model for the IV state based on the concept of the exciton of the finite radius has allowed us to understand the most of the effects observed in lattice dynamics (caused by charge fluctuations and its contribution to the electron-phonon coupling), as well as in magnetic subsystems. A spectrum for the latter is defined by f-electron excitations which are not connected to the charge transfer, but result from the interaction of spin and orbital degree of freedom. In the framework of this model, it is suggested that on each RE ion the ground (g) state is formed, which is quantum mechanically mixed from two initial or 'parent' configurations that correspond to: (1) the totally localized loosely bound f-electron and (2) the delocalized state of this electron, as shown by the equation

$$\alpha|\,\mathrm{f}^6\rangle_{J=0} + (1-\alpha^2)^{1/2}|\,\mathrm{f}^5\mathrm{B}^{\mathrm{f}}\rangle_{J=0} = \Psi^{\mathrm{g}}_{J^*=0}\,, \qquad (16)$$

where α defines the contribution of localized Sm^{2+} states, and B^f describes loosely bound ('excitonic') state of f electron localized near the Sm ion.

It is important that in representation (16) the extent of the delocalization is defined by the conditions of the hybridization of the f-electron with one state or another of the electron subsystem of the crystal, and does not correspond to the total exit of the electron from the close vicinity of a particular ion. This way, an excitonic state of finite radius is formed near each RE ion due to hybridization; the corresponding state of a loosely bound electron may be described by a double well potential, as shown in Fig. 14.

The total wave function of the new IV ground state (16) possesses its own excitation spectrum, which mainly consists of two sets of states which are related to a charge redistribution (between excitonic and localized states), or to the change in mutual orientations of spin and orbital moments. The latter type of state is just the background for the properties of the 'resonance mode' which is, in fact, excitation from the true ground state of the total wave function Ψ_g (16) of the IV ion (from $J^* = 0$) to the first excited state, differing by the mutual orientation of spin and orbital moments ($J^* = 1$). Both of these states belong to the full (true) wave function and therefore have a long lifetime, due to which we have a low width of the resonance mode in the neutron spectra. At the same time, the delocalization extent of the electron $1 - \alpha^2$, that is, the probability of it being found in the external well (see Fig. 14), determines the extent of the energy decrease for the spin-orbital excitation $J^* = 0 \to J^* = 1$ with respect to a basic energy of 36 meV for the totally localized ($\alpha = 1$) configuration, that is, f^6.

We have no chance to discuss here many interesting details of the above approach. But in general we can mention that, based on this excitonic model, it appears possible to understand and quantitatively describe anomalies of electron–phonon interaction (for details, see review article [79]) and the dependence of the energy of the resonance mode on the average valence (see Fig. 12b). In addition, the source of the formation of the anomalous form factor for the resonance mode has been suggested. Later on, based on this approach, the dispersion of the energy and intensity of the magnetic excitations (resonance mode and intermultiplet transition ($J = 0 \to J = 1$) in Sm(Y)S [69] was quantitatively described. Recently, it appears that a new set of data for Eu-based systems may also be considered for the general presentation of the excitonic model (see Section 3.4.3).

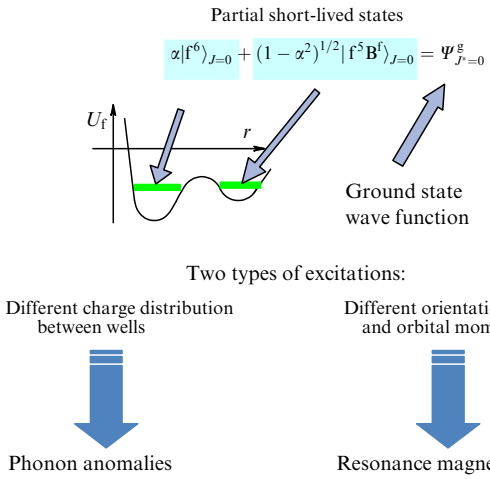

Figure 14. Presentation of the double well potential U_f for a loosely bound electron of the Sm-ion f-shell shared between configurations f^5 and f^6 according to the excitonic model [54].

It is important to note that the approach presented provides a deeper insight into the physics of the effects which were initially presented as a consequence of the simple symbolic equation (15). Also important is that this approach has been formulated in the form presented above based on the results of detailed neutron-spectroscopy studies.

Recently, renewed interest in the properties of SmB_6 have risen due to the development of the concept of the 'topological insulator' and the consideration of this substance as a representative of this class of materials. A new neutron spectroscopy study of the same single crystal [84] was carried out on a time-of-flight spectrometer belonging to the modern generation of such instruments with enhanced capability. The instruments of this class allow, first, the scanning of reciprocal space using single crystals (a multi-pixel detecting system with a large solid angle) and, second, obtaining a large range of momentum transfer (by optimization of the ratio between the energy of excitation studied and incoming neutron energy for a multi-pixel detecting system).

As a result of this study, it appears possible to establish important properties of the resonance mode (14 meV, steeply decreasing form factor). In Fig. 15b, the experimental data of [84] are presented as a colorized map of intensity in the [100]–[011] plane of the reciprocal space, which includes all three main symmetry directions, and in some extra segment the point X at $\mathbf{Q} = (0, 0.5, 1)$ is also shown (corresponding to $\mathrm{X} + \mathbf{G}$). In Fig. 15a, the results are shown of the previous study [62] of the same excitation as a detailed intensity map around the point R for ($\mathbf{Q} = (0.5, 0.5, 0.5)$, $|\mathbf{Q}| = 1.3$ Å^{-1}) of the same plane of the Brillouin zone. The use of the three-axis spectrometer allowed the **Q**-dependence of the form factor to be studied in detail and the strong anisotropy of 14-meV excitation reflecting the concentration of the scattering intensity along direction [111] to be discovered. The X point $\mathbf{Q} = (0.5, 0, 0)$ in that study appears to be out of the range of experimental access.

The opportunity realized by new time-of-flight spectrometers permitted observing the same signal of the resonance mode additionally at two X-type points (which corresponds to different zone boundaries along the direction [100]). In the first and second Brillouin zone, the measured intensities are in

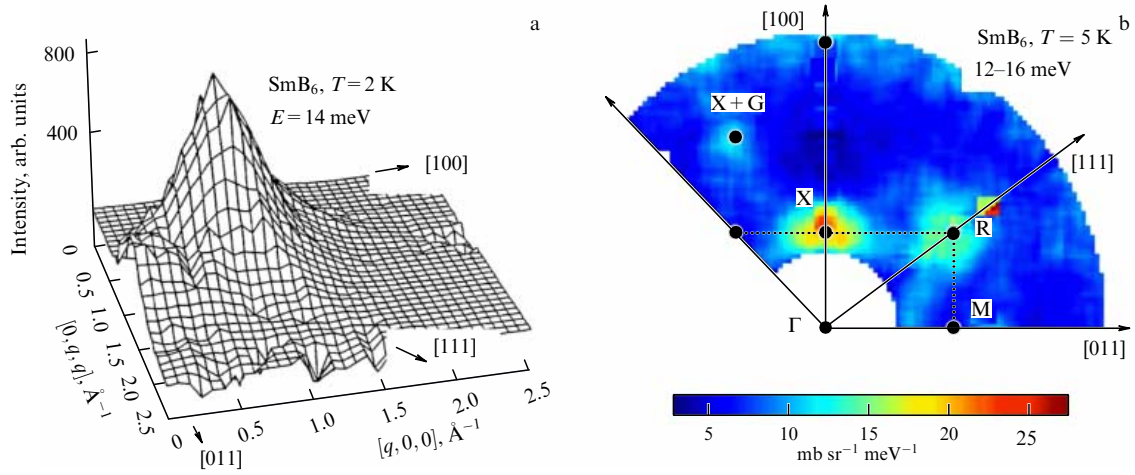

Figure 15. Intensity 'maps' for the resonance mode at 14 meV in the momentum transfer space of the first and second Brillouin zones of SmB_6 single crystal measured at low temperatures. (a) The detailed profile of the intensity from the three-axis spectrometer [62] 2T (LLB, Saclay) data. (b) Colorized map for the intensity in the energy range 12–16 meV [84], data form time-of-flight spectrometer SEQUOIA (SNS, Oak Ridge). It is seen that signals of different intensities are present at three points of the reciprocal space X, X + **G** (**G** is the reciprocal lattice vector), and R. The white circle area is not available for the present energy transfer range for kinematic reasons.

accordance with the Q-dependence of the form factor from [62], which results in higher intensity at the X-point and much lower intensity at X + **G** (**G**-reciprocal lattice vector). The reproduction of the signal in the different zones testifies to the existence of correlation effects. This new experimental result can be treated as an indication of the important role of band effects [84] in the formation of the resonance mode, considered in the excitonic model [54] from a purely single site point of view.

Before finishing the part devoted to the physics of the IV state, it is necessary to mention the quite extended study of the Ce-based IV system — intermetallic compound CeNi. These results still need analysis and discussion in connection with other related data, but some of them can be considered to be pioneering.

3.2.3 Phonon softening and spin gap in CeNi. The study of CeNi (average valence of Ce is in the limits 3.10–3.15 depending on the temperature) should be mentioned here because of the number of original results presented in [72, 73, 75, 77, 78].

(1) We have been lucky to observe for the first time clear evidence of the influence of the IV state on the lattice dynamics of this system based on cerium. Before this, such effects had not been observed, and some opinion was even developed that the absence is not due to the case but is a consequence of charge fluctuation much faster than spin in Ce-based IV systems [85]. This means that for such systems, in, fact, the quasi-adiabatic approximation is realized at the charge fluctuation energy for phonon frequencies. Due to this, the frequencies of the charge fluctuations appear to be above the phonon spectra frequencies, $\hbar\omega_{\rm el} \gg \hbar\omega_{\rm ph}$ (it was substantiated that for Sm-based systems this is not the case: spin and charge fluctuations are of the same range of frequencies), and therefore there is no effect on phonons.

Our measurements of the acoustic and lower optic phonon dispersion (in total for this system 12 nondegenerative phonon branches should exist) carried out on CeNi single crystals in a large range of temperatures and in comparison with its neighbors — LaNi and PrNi — clearly show [75, 78] anomalous softening and anomalous temperature dependence of frequencies for a number of phonon modes. Some experimental data are presented in Fig. 16, where substantial softening (up to 20%) of longitudinal phonon modes close to the Brillouin zone boundary can be seen, in comparison with the structural analogue LaNi, as can temperature anomalies for these boundary phonons in CeNi. This study disproves the idea of the 'exclusive right' to phonon anomalies induced by the IV state for the Sm-system.

(2) In the magnetic excitation spectra of CeNi,[9] spin gap formation at temperatures below 100 K has been discovered [72, 86]. Along with this, the metallic properties of the substance remain unchanged up to low temperatures, differing from the behavior of another class of systems with spin gaps, well known in the literature under the name 'Kondo insulators'. In the latter systems, the spin gap appears in connection with the metal-to-insulator transition upon a temperature decrease. The gap in the magnetic excitation spectra of CeNi measured by neutrons is of the order of 30 meV; it exists at relatively low temperatures (below 100 K). Upon temperature increase, broad ($\Gamma/2 \sim 15-20$ meV) quasielastic scattering starts to dominate in the spectrum. Corresponding experimental results are presented in Fig. 17.

The presented temperature driven modification of the magnetic spectrum is typical for the Kondo insulators (see Section 3.3). The average valence of Ce in CeNi (around +3.12 at $T = 80$ K) considerably deviates from the integer value in the full range of temperatures studied, which is more typical of intermediate valence compounds. In publication [72], the influence on magnetic excitation spectra of 'negative chemical pressure', that is, an increase in the distance between atoms in the crystal lattice of CeNi under the effect of substitution of nonmagnetic La to Ce has been studied. As was shown in [87], an increase in the La concentration results in a decrease in the Ce valence and near Ce/La ~ 1 the Kondo

[9] These experiments were carried out on poly- and single crystals prepared from the weak neutron scattering nickel isotope (^{60}Ni), which allowed the phonon contribution to the spectra measured by neutron scattering to be minimized.

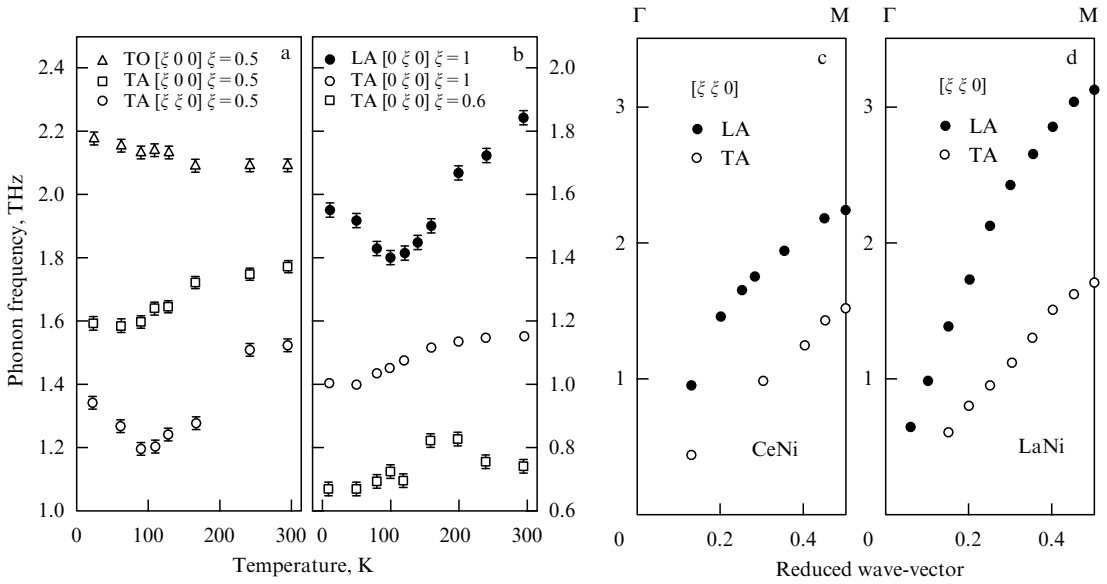

Figure 16. (a, b) Energies of acoustic (longitudinal — LA and transverse — TA) phonons in CeNi as a function of temperature close to the Brillouin zone boundary (from the work [76]). (c, d) Energies of LA- and TA- phonons as functions of a reduced wave vector at $T = 295$ K for CeNi and LaNi (from [75]).

regime can be realized. Our study showed the suppression of the spin gap upon increasing the concentration of La to 0.6; the gap is replaced by the quasielastic spectral function in combination with the inelastic contribution. A further increase in the La concentration results in the formation of a spectral structure typical for Kondo systems, that is, the presence of obvious inelastic peaks similar to the CEF ones (see Section 3.1). Thus, based on the system CeNi, the transition from spectra with a large spin gap (not less than 30 meV) corresponding to the singlet ground state at low temperatures and broad quasielastic signal at $T > 100$ K to the spectrum with dominating CEF single ion effects has been realized.[10] Earlier, a similar transformation had been produced by a less direct way — by the substitution of the second component in the binary intermetallics for the sequence of $CeIn_3 - CeSn_3$ compounds [88].

(3) Detailed measurements with a single crystal sample [77] have shown two relatively narrow peaks in the spin gap at low temperatures in the energy range of 20–37 meV, with q-dependence of intensity (strong) and energy (relatively weak) as shown in Fig. 18. An increase in the temperature resulted in the loss of its intensity and final disappearance together with the spin gap [86]. The existence of these peaks was presumed in the first powder measurements (two peaks are shown in Fig. 17 by firm lines), but the systematic study of the single crystal only provided clear evidence of its existence. The double peak structure may be considered a specific manifestation of the excitation of the resonance mode type in the 'magnetic' sublattice of the same type discussed above for PrNi (same structure), that is, a sublattice with two coexisting interacting magnetic ions in the primitive cell.

[10] This effect demonstrates the essential difference between the reaction of the magnetic excitation spectrum of CeNi upon substituting nonmagnetic La for Ce in Ce(La)Ni with respect to a similar substitution by nonmagnetic Lu for the YbB_{12} spectra. In the latter case, the spin gap is practically unchanged up to a high enough concentration (around 0.5) of Lu in the RE sublattice (see below).

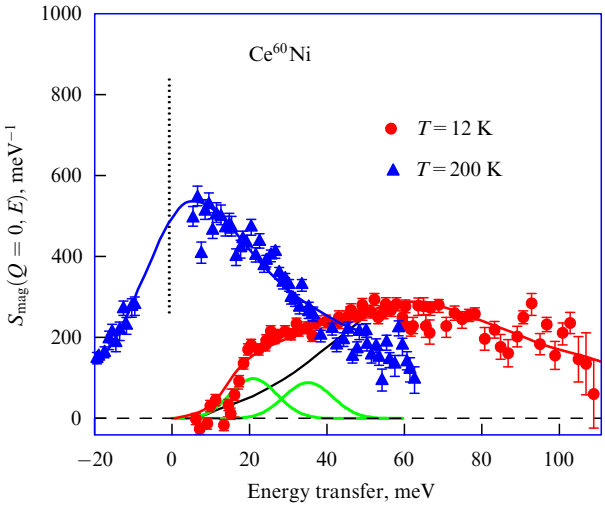

Figure 17. Magnetic contribution to the scattering function for CeNi (from [72]); lines show the fitting by Lorentzians (at $T = 200$ K, only quasielastic scattering is present). The region of the contribution of the elastic nuclear scattering is excluded from consideration.

Measurements of CeNi samples with nonmagnetic substitution impurity (La) in the RE sublattice, in particular, the single crystal $Ce_{0.85}La_{0.15}Ni$ [78], have shown that violation of the coherence in the magnetic sublattice has a considerable influence on the character of excitation spectra and other properties. The first clear effect is the evolution of phonon frequencies, and in this case magnetovibration interaction may be partly involved. For CeNi, the detailed study of the temperature effects on lattice parameters, inter-ion spacing, and average valence, in connection with the magnetic spectrum structure, has been done as well [86]. The conclusion was that some correlation effects in CeNi do exist and influence the temperature dependence of the above parameters at temperatures below 150 K. Thus, one can assume that in the CeNi IV-system (average valence 3.10–3.15, which

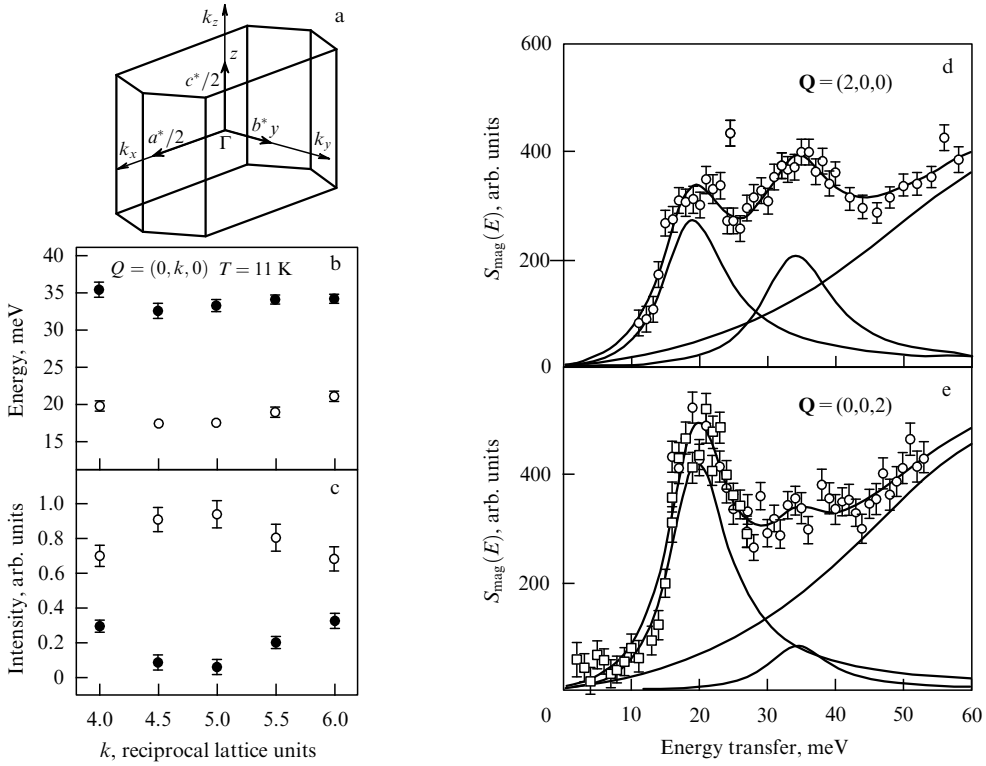

Figure 18. Some results of the magnetic neutron spectroscopy study of single crystal CeNi using a three-axis spectrometer [77] at $T = 11$ K. Schematic presentation of the Brillouin zone (a). Dispersion of energy (b) and intensity (c) for two peaks near the gap edge; real experimental scans at different Brillouin zone centers (d, e). Lines show the results of fitting by three Lorentzians.

is not a small value for cerium) cooperative effects are present, which probably arise from the same kind of interaction which results in induced magnetic ordering in singlet ground state system PrNi or the observation of dispersive magnetic modes in Sm(Y)S.

In a general sense, it is necessary to note that CeNi, along with $YbAl_3$, $EuCu_2Si_2$ (see Section 3.4.3) and, perhaps, some other compounds, can be designated as a valence-unstable metal with a spin-gap type of ground state. This is the specific difference with respect to Kondo insulators, which are systems where the spin-gap formation is closely related to the metal–insulator transition. In spite of the quite large amount of experimental information obtained, we could not find a correspondence between a set of features of CeNi spectral characteristics and any theoretical approaches available to us. Therefore, further experiments have been postponed until the appearance of an adequate theoretical model which will allow us to choose where to concentrate our efforts.

3.3 Kondo insulators: 'classical' example of YbB_{12}

One of the group of IV compounds, as has been mentioned above, demonstrates combined metal–insulator and magnetic–nonmagnetic state transitions upon a temperature decrease under the condition of f-electron instability. A 'classical' example of such behavior is presented by the widely studied system of this class — the compound YbB_{12}. In Fig. 19, the dependences of the effective number of charge carriers

$$N_{\text{eff}} = \frac{\Delta n}{m^*} \propto \int \sigma(\omega, T)\, \mathrm{d}\omega - \int \sigma(\omega, T = 300\ \text{K})\, \mathrm{d}\omega$$

and the value of the effective static magnetic moment $\mu_{\text{eff}} \propto \sqrt{\chi(T)T}$ on temperature are presented. Both parameters are calculated using the corresponding dependences of the dynamical conductivity [89] and magnetic susceptibility [90]. It is seen that suppression of both parameters with decreasing temperature develops in a similar way. This is evidence of the simultaneous opening of the charge and spin gaps [91], which takes place against the background of

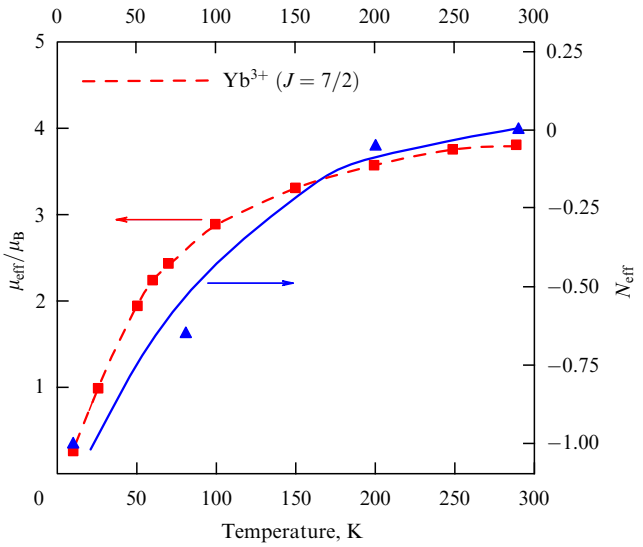

Figure 19. Experimental temperature dependences for the effective magnetic moment on Yb-ion (μ_{eff}) and effective number of charge carriers (N_{eff}) in YbB_{12}.

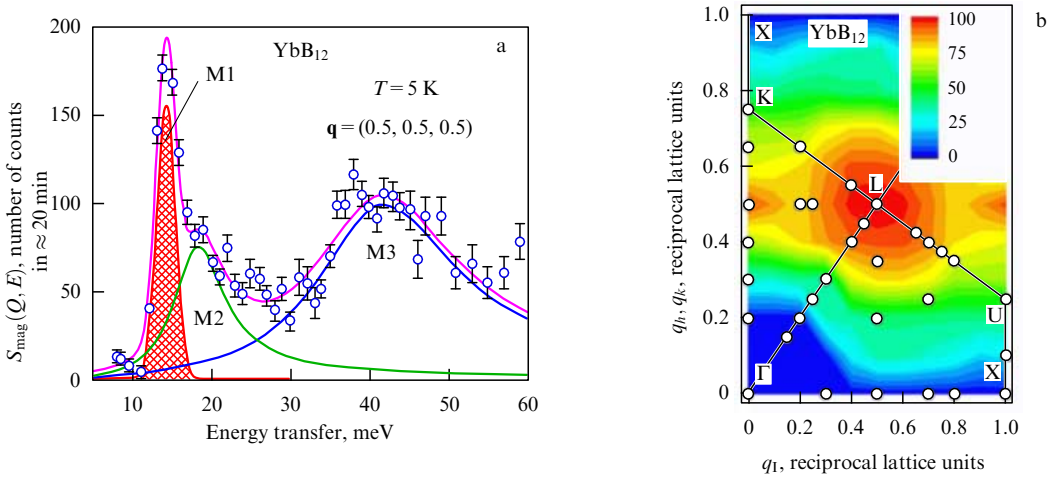

Figure 20. (a) Spectrum of magnetic excitations for YbB_{12} single crystal measured on a three-axis spectrometer with polarization analysis at $T = 5$ K, at $\mathbf{q} = (0.5, 0.5, 0.5)$ (L-point for the direction (ζ, ζ, ζ) at the Brillouin zone boundary). Circles — experiment, lines — fitting calculations by three Lorentzians. The hatched area corresponds to the resonance mode. (b) Map of the intensity (in arbitrary units) of the 15-meV peak at $T = 5$ K corresponding to a plane segment of the Brillouin zone. Circles denote the points in **q**-space where the corresponding spectra have been measured in analogy with (a). (From [100].)

(2.95(5)) valence, only slightly deviating from the integer value.

Historically, the class of systems with such properties has the general title Kondo insulators; it was later discovered from further studies that the physical background of the effects observed may be quite different in different systems and might not even be directly connected to the Kondo effect. Nevertheless, in many review articles [92–94] the group of systems based on Ce, U, Sm, Yb, and, in particular, SmB_6, SmS (IV phase), etc, are considered members of the 'family'.

The first results of neutron spectroscopy studies of polycrystalline samples of the YbB_{12} Kondo insulator were published by two independent experimental groups in 1998 [95] and in 1999 [91], providing a reliable database for subsequent work. During the following years, we carried out comprehensive studies of the atomic lattice and magnetic excitations, both cooperative and single site. Special attention was focused on the effects of such factors as violation of the coherence in the RE-sublattice, or electron doping [96–105]. These influencing factors allow the range and specifics of the interactions which are responsible for the formation of the specific properties of the Kondo-insulator state to be defined more clearly. Let us consider the main results of the above mentioned work.

3.3.1 Magnetic excitations. Experimental results of measurements with powder and single crystal samples, including measurements with polarized neutrons [98–100], allow us to establish undoubtedly the structure and character of the temperature evolution for the magnetic excitation spectrum of YbB_{12}. This makes sense in connection with the question of the origin of the joint transition from a magnetic metal to nonmagnetic narrow-gap semiconductor realized in this compound.

The magnetic excitation spectrum from the ground state of YbB_{12} constitutes the aggregate of dispersive excitations (Fig. 20), two of which with maxima at 40 meV and 20 meV (M3 and M2) possess a considerable intrinsic width ($\Gamma \approx 5-10$ meV), but one, at the energy of 15 meV (M1), possesses, on the contrary, a vanishing width and is localized in q-space close to the direction $(q, 1/2, 1/2)$ with the maximum at the point $(q = 1/2, 1/2, 1/2)$, that is the L-point of the Brillouin zone [98, 99]. The same point corresponds to the minimum of the energy dispersion of this low energy excitation. These facts correspond to the idea of an antiferromagnetic character of correlations (possibly two-dimensional) responsible for the observed q-dependence of the parameters of 15-meV excitation.

The above mentioned magnetic excitation (M1) may be classified as a resonance mode according to its characteristics. It is also clear that this resonance mode exists in the spin gap, while two other excitations (M2, M3) are located above the gap, indicating a gap size of about 20–25 meV. The formation of the spin gap at low temperatures is proved by the absence of any evidence of quasielastic scattering under these conditions, which is generally present in heavy fermion or intermediate valence compounds. Our special measurements with a rather high (with respect to the scale of spin fluctuation expected for this class of compounds) energy resolution (≈ 0.1 meV) [96] did not show any evidence of quasielastic scattering for YbB_{12} in the temperature range from 5 K to 40 K. When the temperature exceeds this level, the quasielastic signal does appear and increases its intensity fast, reaching the maximum value at $T \sim 100$ K; the width of the peak, on the contrary, does not greatly vary and is large enough just from the moment the signal appears, being around 15–18 meV (FWHM).

The temperature range of 50–80 K where the quasielastic signal is formed corresponds to the region of radical transformation of the excitation spectra, which is illustrated in the general sense in Fig. 21. Transformation is described in [99, 101] as the disappearance of all three inelastic peaks (M1disappears faster than others) and their simultaneous replacement by one broad quasielastic excitation and another inelastic peak at an energy of around 22 meV (Mh in [101]) without no any observable q-dependence. In such a way, the high-temperature ($T > 80$ K) spectrum of magnetic excitation is characterized by quasielastic and inelastic peaks originating at a single site. A quantitative interpretation of this spectrum can be related to highly dampened

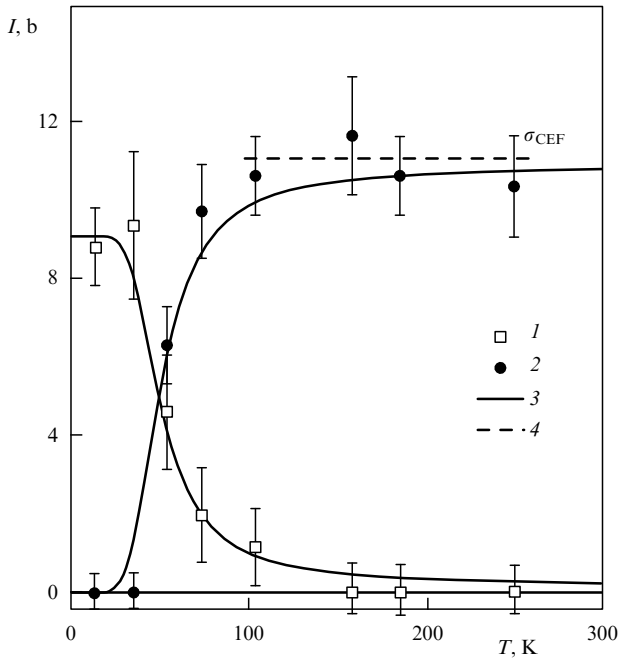

Figure 21. Temperature dependence of the partial contributions (see Figs 20 and 22) to the intensity of the magnetic neutron scattering on YbB_{12}: *1* — low temperature regime, sum of M1, M2, M3; *2* — high temperature regime, sum of M_h (presenting peak at 22 meV, see Fig. 22b and [101]) and quasielastic signal; *3* — calculation corresponding the high extent of the degeneracy of d-states in the conduction band according to the representation of [106] based on the single-site origin of the excitation spectrum; *4* — total intensity of the magnetic neutron scattering related to the transitions between CEF-split levels of Yb^{3+}. (Taken from [101].)

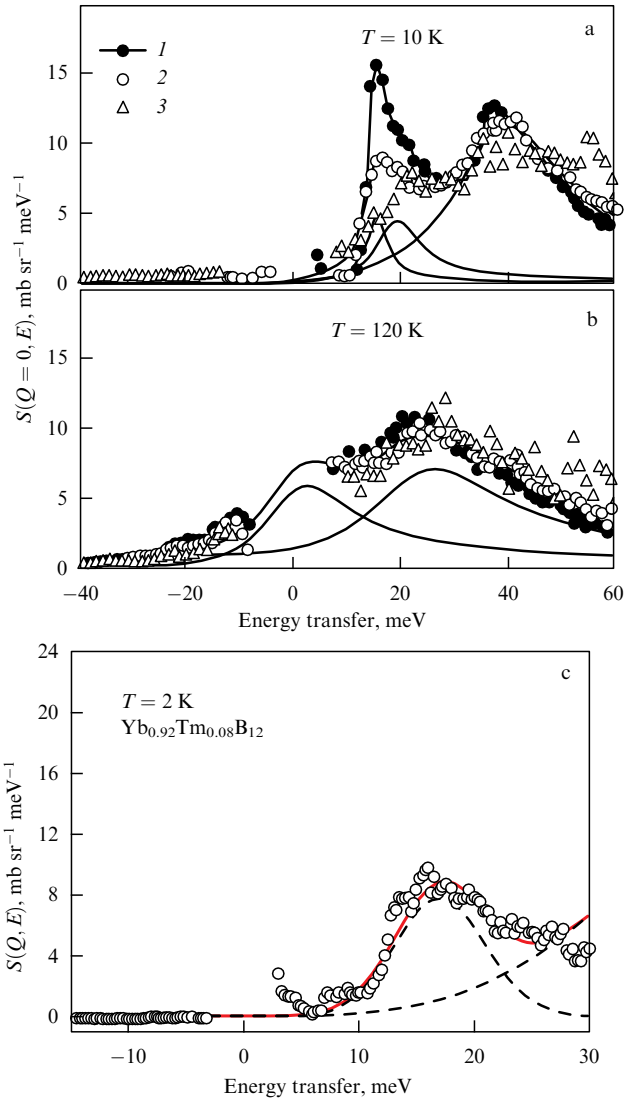

Figure 22. Magnetic excitation spectra of $Yb_{1-x}Lu_xB_{12}$, $x = 0$ (*1*), 0.25 (*2*), 0.75 (*3*) at temperatures $T = 10$ K (a) and $T = 120$ K (b). Lines represent the fitting of the scattering function by Lorentzians (including a quasielastic one at $T = 120$ K); the temperature factor is included in the fit. (From [101]). (c) Magnetic excitation spectra of the Yb ion in $Yb_{0.92}Tm_{0.08}B_{12}$ at temperature $T = 2$ K. Lines show the fitting of the scattering function by Lorentzians positioned at energies of 18 meV and 40 meV; the temperature factor is included; the resonance mode at 15 meV is absent [compare with (a)]. (From [103].)

CEF[11] excitations arising from the splitting of multiplet $J = 7/2$ for Yb^{3+}, which corresponds to the typical picture for heavy fermion regime (see Section 3.1). It is important that only in this temperature range does the transition (upon a temperature decrease) take place from metal to a narrow gap insulating state with the gap of the order of 10 meV in the conduction electron density of states.

Studies on the influence of nonmagnetic isoelectronic [97, 101] or nonisoelectronic (changes to d-electron configuration) defects [102] (that is, replacement of Yb by Lu or Zr, respectively) have allowed us to establish a number of important facts. Violation of the coherence (substitution Lu to Yb up to a considerable value, above 50% [101]) (Fig. 22) influences mostly the parameters of the resonance mode and does not really change the gap character of the low temperature spectrum or its temperature evolution. It appears that at temperatures above 120 K all spectra are identical to the ones shown in Fig. 22b. Nevertheless, a relatively small amount (around 20%) of nonisoelectronic (Zr) impurity [102] results in the total suppression of the resonance mode, partial filling of the gap, and a substantially smoother transformation of the spectral function to the high temperature regime shape which resembles a thermodynamically driven one.

Consequently, in YbB_{12} the formation of a nonmagnetic and cooperative (dispersion of excitations!) ground state takes place, with the specific excitation spectra which include a resonance mode and spin- and charge gapes. The spin gap most probably has a local, not a coherent, origin. This observation means that local as well as cooperative interactions should be considered against the background of the formation of such an excitation spectrum.

In a recent publication [103], the influence of the isoelectronic but *magnetic* impurity (Tm^{3+} ion with a triplet CEF ground state Γ_5 which carries a magnetic moment of about 4.7 μ_B, which is considerably larger than the magnetic moment of the Yb^{3+} ground state Γ_8 which is close to only 2.2 μ_B). It appears that less than 10% of a Tm-impurity is enough (see Fig. 22c) to suppress the resonance mode, and 15% Tm results in the partial filling of the spin gap even at 2 K. However, a transition to the high temperature regime remains quite narrow in temperature, not as in the case of $(YbZr)B_{12}$. The observed effect of suppression of the 'resonance' mode and gap through the isoelectronic magnetic impurity may be a result of the formation of magnetic

[11] The scale of CEF splitting for Yb^{3+} is of the order of 12 meV from the estimation based on INS experimental data for 10% impurity of Er^{3+} ion in YbB_{12} [97].

defects in the RE sublattice, which destroys the Kondo cooperative state for Yb-ion f-electrons and conduction electrons. Apparently, this effect serves as the most radical way to destroy the formation of the Kondo-insulating state due to some kind of 'undercompensation' of magnetic moments of localized f-electrons of Yb ions.

The resonance mode in YbB_{12} appears to be different in physical origin with respect to the ones observed in Sm-based systems. Its form factor inYbB_{12} corresponds to the standard one for the f-electron J-multiplet [96, 98], its q-dependence, and repetition in the reciprocal space, giving evidence of the cooperative origin of the excitation due to the exchange interaction. To understand this, several theoretical models have been suggested: one considers the balance between CEF effects and exchange under the condition of hybridization interaction [106], another one basing on the gap structure of the spectrum [107], and one is based on the effects of dimerization in the Yb-ion magnetic sublattice [108]. But for the explanation of the observed change in regimes in a very narrow temperature interval (compared with other characteristic physical parameters, such as excitation energy and width of the quasielastic peak), no significant models have been suggested, except the assumption of the existence of a 'hidden parameter' which is responsible for the 'changeover' of the system from one regime to another.

3.3.2 Specifics of the lattice dynamics. The idea of the existence of a 'hidden parameter' responsible for the sharp transition in temperature decrease from the spin-fluctuative — similar to heavy fermion regime — to the singlet ground state with the spin gap gives rise to a search for possible anomalies in the lattice dynamics which can be considered a system of excitations external with respect to the spin-electron one, but with some interconnection probably.

The lattice dynamics have been studied experimentally by different neutron scattering techniques. The density of vibration states has been studied on the level of a partial contribution (two types of atoms: RE and boron) using the method of 'isotope contrast' developed at the Kurchatov Institute [79]. Extensive studies of the dispersion relation (limited by the frequency of about 10 THz) have also been realized [104]. Based on the above results, the calculations have been carried out using a model of force-constants. This allowed establishing the strong hierarchy of inter-ion (RE – RE, RE – B, B – B) interactions: heavy RE ions appear to be weakly connected in the three dimensional network based on B_{12} cubooctahedrons. Later, a DFT–LDA *ab initio* calculation of the lattice dynamics [109] was developed. In this work, the strengths and weaknesses of this approach with respect to the particular structure were shown. The calculated density of states in the boron vibration frequency range almost ideally corresponds to the experimental one, but this is not the fact for low frequencies related to RE-ion vibrations.

No detectable temperature anomalies for the energy of phonon branches were found in the experiments. Nevertheless, an unusual behavior of the intensities of acoustic phonons near the Brillouin zone boundary with an energy of about 15 meV (close to the energies of the resonance mode (M1) and another 'over-gap' excitation peak (M2) located at about 20 meV) has been found in detailed study [105]. The effect observed has been localized at some selected values of the phonon wave vector (presumably near the zone boundary) and determined for phonon polarization symmetrically identical to magnetic dipole excitations.

This effect shows the existence of certain interactions between magnetic and vibrational subsystems and provides some evidence of the possibility for a phonon subsystem to influence the formation of the ground state of YbB_{12}. It is interesting that intensity renormalization is observed instead of the renormalization of the frequencies, as was illustrated in review article [79] (see Fig. 20 in that article). This may be a demonstration of mode to mode hybridization under the specific condition of the strong hierarchy of inter-ion interactions in a multicomponent system with high crystal symmetry. These problems are discussed, in particular, in a review devoted to specifics of the boride lattice dynamics [79].

The YbB_{12} example shows that in-depth and comprehensive inelastic neutron scattering studies combined with other methods allow us to get quite unexpected and nontrivial results on the front line of experimental research in the field of SCES physics.

3.4 Long range magnetic order in heavy fermion and intermediate valence systems

In the overwhelming majority of cases, long range magnetic order (LRMO) for rare earth compounds is based on interaction between local magnetic moments of RE ions. Exceptions from this trend are related to cases of compounds with transition metals, oxides in particular, some iron-pnictides, chalcogenides, which recently became a subject of intensive studies due to the discovery of superconductivity with relatively high critical temperatures [110, 111], and a few examples of intermetallic compounds. Thus, in most cases LRMO in rare earth intermetallic compounds means the spatially ordered coherent state of well-defined magnetic moments with a magnon type excitation spectrum.

It can be thought generally that disruption of the 'normal' state of the localized f-electron moment by the switch on of hybridization with band states and consequently the appearance of spin fluctuations (see above, Sections 3.1, 3.2) additionally to CEF-effects specific to intermetallic systems should result in the breakdown of the spatially coherent state of well-defined magnetic moments (that is, LRMO). The obvious basis for such a vision is the scale of the Kondo temperature (T_K) coincident with the scale of temperatures of magnetic ordering which are not very high. This is true for most cases: heavy fermion systems ($CeAl_3$, $CeCu_2Si_2$, $CeCu_6$, etc.), intermediate valence compounds ($CePd_3$, CeNi, etc.), and Kondo insulators ($Ce_3Bi_4Pt_3$, YbB_{12}, SmB_6) possess a nonmagnetic ground state frequently treated as an analogue of the nonmagnetic singlet.

However, up now a number of cases are known to have been considered exceptions to this general view. They are very interesting from the point of view of analysis of 'exotic' conditions for the emergence of long range order. Below, we will consider some variants of competition and the coexistence of LRMO and spin fluctuations.

3.4.1 Magnetic ordering in systems with heavy fermions. The transition from the heavy fermion state to the magnetically ordered (antiferromagnetic as a rule) one was experimentally discovered (more than 20 years ago) for a number of RE intermetallic compounds based on Ce (mainly) and Yb as well, which belongs to the large family of REM_2X_2 ('1–2–2' in what follows) systems. In fact, in experiments, it was observed that with decreasing temperature typical evidence of the formation of the heavy fermion state was developed

(logarithmic increase in resistance, high enough Sommerfeld coefficient in heat capacity), but on approaching some critical temperature (T_N) of the order of 10 K, a phase transition was observed to antiferromagnetic LRMO.

In some sense, Cerium- and Ytterbium-based systems can be treated as 'mirror-like' analogues from the point of view of f-electron instability. In the first case, on the f-shell one loosely bound electron is present, whereas in another one a loosely-bound 'hole' exists. Examples of such systems are $CeCu_2Ge_2$ ($T_K \sim 8$ K, $T_N \sim 4$ K), $CeAg_2Ge_2$ ($T_K \sim 3$ K, $T_N \sim 7$ K), $CeAg_2Si_2$ ($T_K \sim 5$ K, $T_N \sim 10$ K) [112], $CePd_2Si_2$ ($T_K \sim 9$ K, $T_N \sim 10$ K) [113], and a number of others, based on Ytterbium: $YbAuCu_4$ ($T_N = 0.6$ K), $YbPdCu_4$ ($T_N = 0.8$ K), $YbBe_{13}$ ($T_N = 1.3$ K), YbPd ($T_N = 0.5$ K) [114, 48]. Uranium compounds such as U_2Zn_{17}, URu_2Si_2 serve as clear representatives of actinide-based heavy fermion systems with antiferromagnetic ordering [115]; for the latter system. the final transition to the superconductive state takes place ($T_N \sim 17$ K, $T_c = 1.2$ K, with a high value of the Sommerfeld coefficient (for $T > T_N$): 180 mJ mol^{-1} K^{-2}).

Studies of magnetic excitation spectra for these and some other compounds have been carried out by inelastic neutron scattering [48, 112–117]. The experiments allowed us to get a clear detailed presentation of the features of magnetic excitation spectra which are identified as typical for heavy fermion systems. The character of behavior of parameters for quasielastic spectral components close to and below the temperature of transition to the ordered state was also discovered. The above results are related to the generalized phase diagram based on the ideas of Doniach [118]. Let us consider in more detail the cerium-based compounds; corresponding results of neutron studies are presented in [112, 113, 116, 117].

Neutron spectroscopy allows us to analyze two energy ranges in the excitation spectrum: (i) excitations related to the transitions between sublevels of the ground state multiplet (e.g., CEF-split); (ii) excitations resulting from spin fluctuations which considerably exceed the energy scale of thermal relaxation broadening of the ground state of a stable magnetic moment (described by the so-called Korringa law ($\Gamma \sim (0.1-0.01)\, k_B T$). Typical experimental data obtained for Ce-based 1–2–2 systems are shown in Fig. 23 (from [117]) for the inelastic part of the spectra, and in Fig. 24 (from [116]) for the temperature dependence of the quasielastic width.

Peaks are observed in the inelastic part of the spectra (Fig. 23), rather broad (in relation to the usual picture for RE ions with stable f-states split by a crystal field). Such type of spectral function is characteristic for paramagnetic HF systems, such as $CeAl_3$, $CeCu_2Si_2$, $CeCu_6$ (see above, Section 3.1); these peaks are usually associated with excitations, strongly damped by Kondo-type spin fluctuations, between crystal field split levels.

The width of a quasielastic signal (see Fig. 24) defined at temperatures above the magnetically ordered region is in correspondence within the typical temperature dependence and scale of width values for classical HF systems. As temperature decreases and approaches the Néel temperature, the transformation of the line shape of the quasielastic line develops by increasing the contribution of the Gaussian-shaped signal, presumably due to the specific fluctuation preceding the establishment of LRMO. However, below T_N the width starts to decrease steeply, thus never crossing the

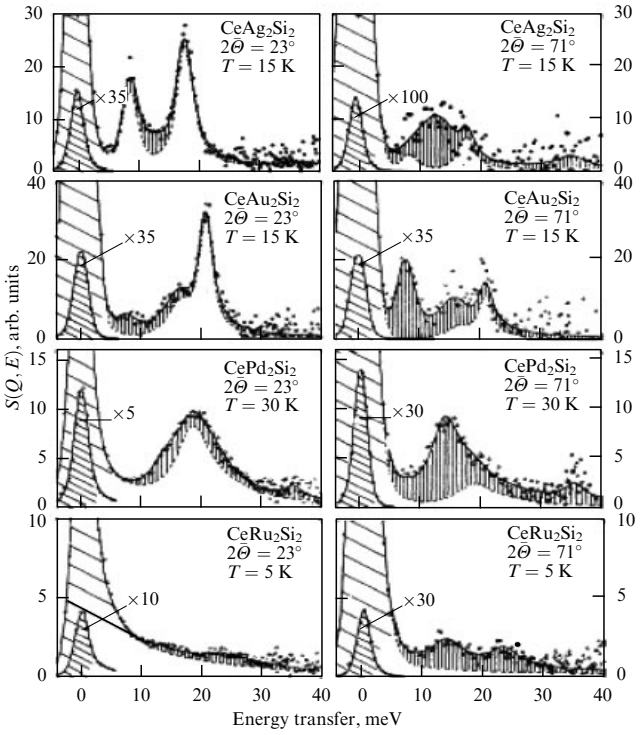

Figure 23. Inelastic neutron scattering spectra for CeX_2Si_2 (X = Ag, Au, Pd, Ru) compounds measured at low ($13° \leqslant 2\Theta \leqslant 33°$) and high ($68° \leqslant 2\Theta \leqslant 74°$) scattering angles. Oblique hatching in the figure indicates the region of the elastic incoherent peak of nuclear scattering. Vertical hatching denotes the contribution from scattering on phonons. Nonhatched area below corresponds to the magnetic contribution to the scattering function. The solid line is the result of fitting taking into account crystal field splitting (for $X = Ag$, Au, Pd). For Ru, it is shown that a pure quasielastic signal is observed in the spectrum. (Taken from [117].)

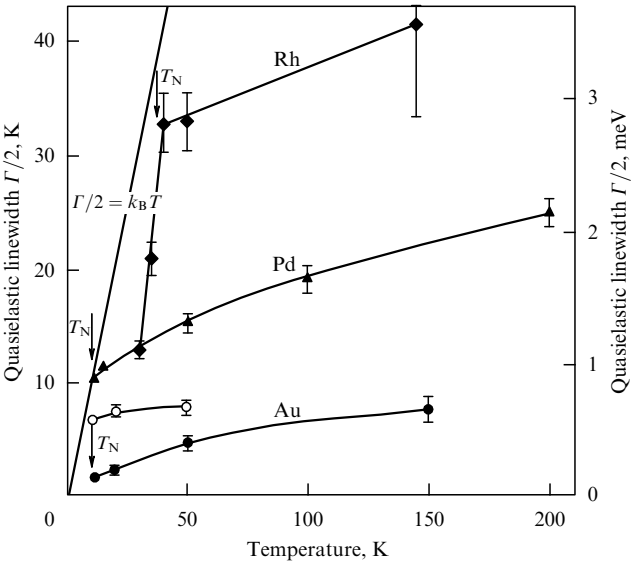

Figure 24. Dependence of the widths of quasielastic lines on sample temperature in the spectra of magnetic neutron scattering for samples of $CeAu_2Si_2$ (black dots — fitting by Lorentzian, white dots — fitting by Gaussian), $CePd_2Si_2$ (triangles), and $CeRh_2Si_2$ (diamonds). Arrows correspond to the T_N. Lines are drawn by eyes. Line $\Gamma/2 = k_B T$ shows the maximum possible for thermal relaxation width. (From [116].)

borderline corresponding to thermal relaxation energy $\Gamma/2 = k_B T$. This fact appears to be substantially different with respect to specific behavior for paramagnetic HF systems, in which case a width $\Gamma_{QE}/2 = k_B T_{sf}(T)$ approaches the constant value order of $T_{sf} = T_K$, crossing the thermal relaxation borderline on decreasing temperature. The intensity of a quasielastic signal also decreases fast below T_N, and apparently at low temperatures (below 2 K) and in the region of low energies (up to 3 meV) the excitation spectrum is defined by soft magnon-like excitations instead of the quasielastic peak.

In [116], an interpretation is suggested of the properties observed for a number of cerium-based systems discussed above. The background for it is Doniach's idea considering competition of the RKKY-interaction with spin-reversal scattering of conduction electrons by f-electrons presented in [118], which is illustrated in Fig. 25.

The dependence of T_K on J_{sf} (exchange integral between 4f- and conduction electrons, J, in Fig. 25) is exponential in character, but for T_{RKKY} there is a quadratic law [42], as shown by corresponding dashed lines in Fig. 25. As a result, an increase in J_{sf} should result in a change to the type of ground state from LRMO to spin-fluctuative (Kondo-regime). Estimations of the value of J_{sf} allow locating the system under consideration CeM_2Si_2 (M = Au, Rh, Pd, Ru) [116], according to a definite order in the presented diagram in the vicinity of the crossing point of J/W-dependences for T_K and T_{RKKY}. Agreement is observed between their experimental characteristics and theoretical line for T_M in the sense of a transition from the LRMO type for the ground state to the spin-fluctuation type. The authors of [116] noted that the decrease observed by neutron diffraction in the ordered magnetic moment with respect to the value for the independent ion is explained precisely by combination of the crystal field effect and the Kondo-effect.

It is necessary to note that the HF-state for the system based on Ce or Yb is usually related to the very tiny deviation of the valence from an integer value. This is confirmed by a large number of results of measurements of X-ray L_3-edge absorption spectra and is typically considered a necessary condition for the application of the perturbation theory for analysis of hybridization effects in the Kondo-regime.

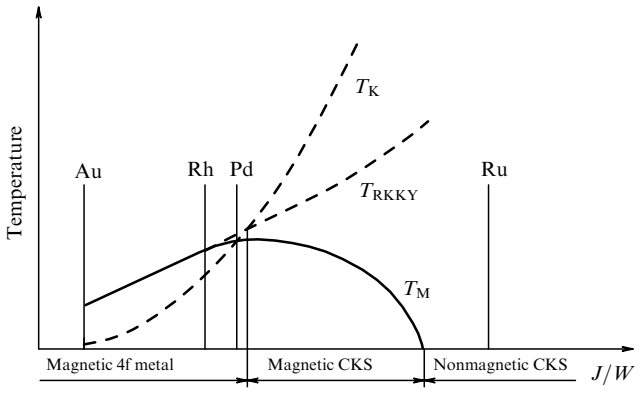

Figure 25. A classification of concentrated Kondo-systems (HF-systems) by the correspondence between two characteristic interactions (indirect exchange and Kondo-like), which are defined by parameters T_{RKKY} and T_K (both presented by dashed lines). T_M (solid line) corresponds to the magnetic ordering temperature (here, $T_M = T_N$), J is the exchange integral (it enters into the definition of T_{RKKY} and T_K) between 4f- and conduction electrons, W is the scaling factor. The vertical lines correspond to the estimated values of the parameter J/W for CeM_2Si_2-systems (T = Au, Rh, Pd, Ru). (From [116].)

An enhancement of the hybridization results in the f-level approaching the Fermi energy and therefore a considerable increase in the charge instability, which appears to be a considerable deviation of the valence from an integer value. In systems of this type, LRMO doesn't normally take place due to fast enough spin-fluctuations with an energy around 10^2 K. This also defines the character of the magnetic response spectrum of such systems (domination of the broad quasielastic signal). Nevertheless, some exceptions to this 'rule' have been observed experimentally and are discussed below.

3.4.2 Magnetic ordering in intermediate valence TmSe. The first case of the combination of 'strong' f-electron instability with LRMO was discovered in the 1980s, with the system under study being TmSe — a semiconductor-like compound with a simple cubic NaCl-type structure. The valence of Tm in this compound is far from integer (≈ 2.58) and is almost temperature independent; nevertheless, below $T_N = 3.45$ K for a stoichiometric composition an AFM-1 magnetic ordering develops [119–121], with a respectively small (in relation to Tm^{2+} or Tm^{3+}; see below) value of the ordered magnetic moment $(1.7 \pm 0.2)\,\mu_B$. An essential circumstance considered to be key for the realization of LRMO under the conditions of strong intermediate valence is the presence of the magnetic moment (m_{eff}) for each competing electronic configuration: Tm^{2+} ($4f^{13}$, $^2F_{7/2}$) $m_{eff} = 4.5\,\mu_B$ and Tm^{3+} ($4f^{12}$, $^3H_6$) $m_{eff} = 7.5\,\mu_B$. The important point is that the crystal field effects for this compound can be not taken into account, as shown in [122], because the energy of spin fluctuations due to the intermediate valence state is higher than the estimated energy of CEF splitting. The existence of the magnetic moments is the key element of some models [123–127] claiming to be an explanation of the properties, first of all — excitation spectra, of this compound.

Magnetic excitation spectra of TmSe are quite unusual for a IV-compound, first of all due to its temperature evolution, studied in a number of publications [123, 128, 129], where powder and single crystal samples were used. In a broad enough temperature range, this is a typical spectrum of the IV-system, which is defined by a relatively broad ($\Gamma/2 = 6$ meV) quasielastic signal (see Fig. 26).

The spectrum is essentially transformed as temperature decreases below 100 K. An inelastic component in the spectrum appears and its energy gradually increases upon approaching 10 meV. Its intensity also gradually increases with decreasing temperature, and simultaneously the width of the quasielastic peak decreases, never exceeding the values corresponding to $\Gamma_{QE}/2 = k_B T$, to the ordering temperature T_N. Below $T < T_N$, the quasielastic signal is not detected; instead, the weak inelastic peak appears in the spectrum at an energy of about 1 meV, which can be related to magnon excitation. Dominating in the spectrum at low temperature, the inelastic component is stabilized at about 10 meV energy transfer; for temperatures up to 50 K, it possesses an observable dispersion of energy and clear modulation of the intensity. Maxima of the intensity and minima of the energy are observed closed to the zone boundary $\mathbf{Q} = (q, 0, 0)$, where q is odd (see Fig. 27). The investigation of the origin of this excitation which demonstrates clear cooperative behavior was considered to be a key element in developing the model of LRMO formation on a background of the IV-state [124, 125, 130].

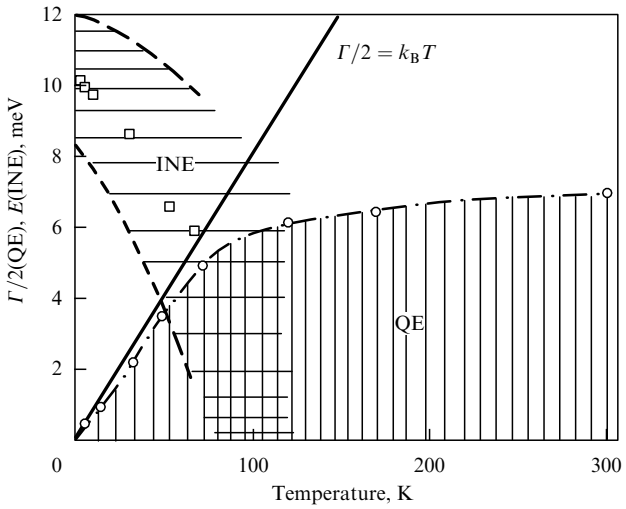

Figure 26. Temperature dependence of the width $\Gamma/2$ of the quasielastic peak (FWHM, circles) and energy E of an inelastic line (squares: the width of the inelastic line is presented by the band of horizontal hatching bounded by the dashed lines) in the neutron scattering spectra of TmSe. (Taken from [123].)

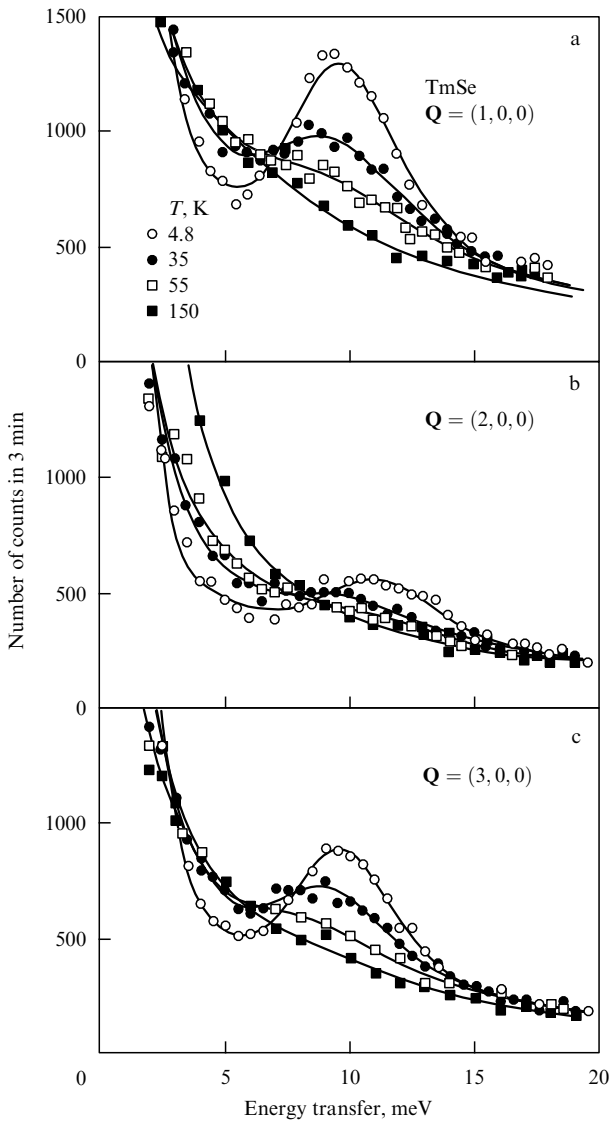

Figure 27. Inelastic neutron scattering spectra for TmSe single crystal, measured with tree-axis spectrometer with $k_f = 3.88$ Å^{-1} ($E_f = 30.5$ meV) near the zone boundaries (a, b) and at the center (c) of crystalline Brillouin zone $\mathbf{Q} = (q, 0, 0)$; (a) $q = 1$, (b) $q = 2$, (c) $q = 3$. Intensity of the peak decreases on temperature increase. The maximum of intensity and minimum of energy correspond to the zone boundary. (Figure from [129].)

An additional study of samples with a high degree of substitution of nonmagnetic La and Y for Tm was carried out in [127]. It was shown undoubtedly that the origin of the inelastic excitation is a single-site ion. Model presentations of the relation among the inelastic excitation, valence instability and magnetic ordering for the ground state of the system have been developed in [124–126], which allowed the interpretation of the ground state as the state resulting from time coherence [12] developing between two competing electron configurations if both carry some magnetic moment. The ordered magnetic moment in this case appears to be several times smaller than any of competing ones, in accordance with the experimental data of [119, 120].

It is necessary to note that Tm (as well as Eu, see below) has several electrons in the f-shell, which is different with respect to the case of Ce or Yb, which for the 3^+-valence case have only one electron or hole, respectively, as was mentioned above. Besides this, the only electrons in the conduction band for TmSe are delocalized f-electrons, hybridized with band (d) states. This peculiarity results in a substantial difference between the TmSe and many other IV-systems with a metallic ground state. The existence of the inelastic peak in magnetic excitation spectra, quite similar in its properties to the resonance mode, observed in Kondo insulator and IV systems (also in HTSC — cuprates and iron pnictides), allows us to consider excitation to be a general feature of strongly correlated systems with spin- or spin and charge gaps.

3.4.3 Antiferromagnetic ordering in $EuCu_2(Si_xGe_{1-x})_2$ intermediate valence systems. The series of solid solutions with substitution Ge for Si — $EuCu_2(Si_xGe_{1-x})_2$ — serve as an example of a system with a combination of characteristic components (mutually exclusive at first glance!) specific to the magnetically ordered, heavy fermion, and intermediate valence behavior of intermetallic compounds. The $EuCu_2(Si_xGe_{1-x})_2$ compound belongs to the broad class of systems with the structure of tetragonal symmetry (I4/mmm) and chemical type $ThCr_2Si_2$ (or $CeAl_2Ga_2$), which is denoted here (and above) as '1–2–2'. The results obtained for this system show that the existing theoretical models describing the combination of the IV-state and the LRMO-state (see above) are not sufficient. Below, the main results of the study of the series of $EuCu_2(Si_xGe_{1-x})_2$ solid solutions by neutron diffraction and spectroscopy, as well as by complementary spectroscopic methods, from [131–135] are discussed in brief.

Earlier, at the initial stage of the study of intermediate valence compound $EuCu_2Si_2$, it was found that when silicon is partly replaced by germanium, in some range of silicon concentrations (around $x \sim 0.75$) the ground state with some evidence of the heavy fermion type is formed [136]. The detailed study of the thermodynamic, magnetic, and transport properties of $EuCu_2(Si_xGe_{1-x})_2$ throughout the entire range of concentration x resulted in a suggestion [131] of a variant of the phase diagram for the low temperature region.

[12] Initially, an alternative model [130] was considered, which also suggests spatial coherence to describe the inelastic peak, but it appears to be uncompatable with experimental data of [127].

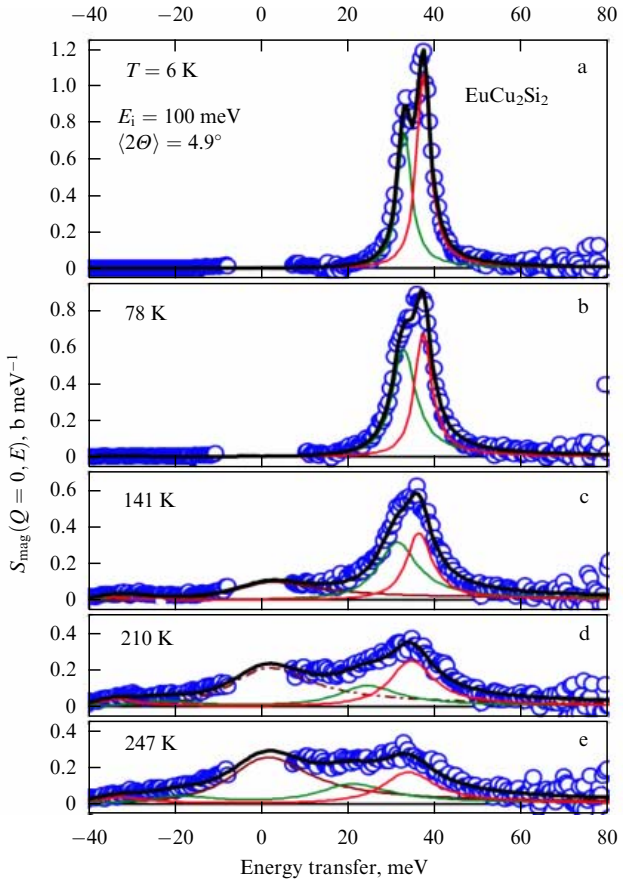

Figure 28. Spectra of the magnetic excitations for $EuCu_2Si_2$ measured at neutron scattering angle $\langle 2\Theta\rangle = 4.9°$; initial neutron energy is $E_i = 100$ meV. Spectra are reduced to $Q = 0$, suggesting a form factor of the double peak equal to the magnetic dipole form factor of spin-orbital transition $^7F_0 - ^7F_1$ for Eu^{3+}. Circles — experiment, curves — fitting by Lorentzians. It is seen that the quasielastic component is present in the spectra starting from field (c) $T = 141$ K. (Data from [132].)

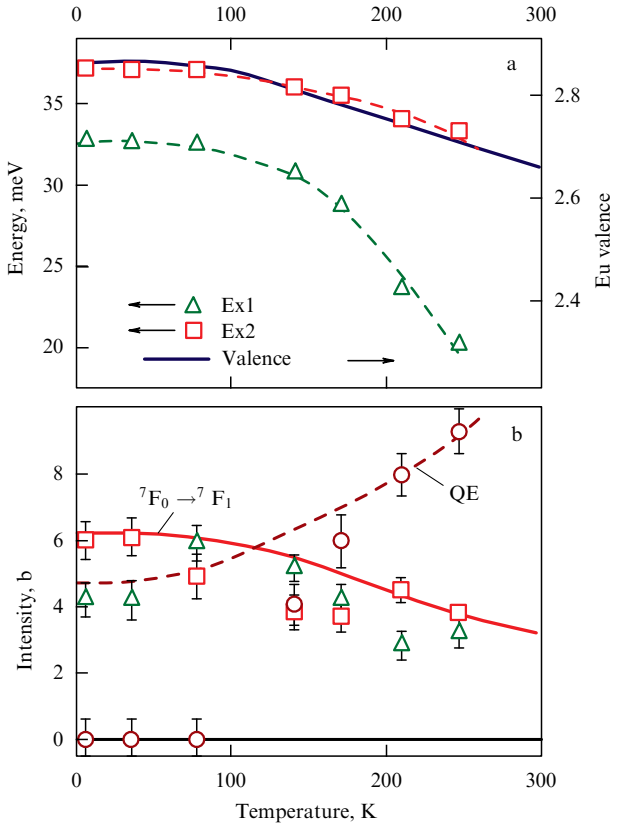

Figure 29. Temperature dependences for energy (a) and integrated intensities (b) for the peaks Ex1 (triangles), Ex2 (squares), and quasielastic peak (circles). In (a) the solid line corresponds to the dependence for average valence; dashed lines are guided by eyes over the experimental points. In (b): solid line — intensity calculation for the hypothetical peak of the $^7F_0 - ^7F_1$ transition of Eu^{3+}; dashed line — calculation for the hypothetical peak of quasielastic scattering on Eu^{2+} which takes into account the temperature dependence on the average valence. (Data from [132].)

One of the main result is the clear indication of the existence of a magnetically ordered ground state, presumably an antiferromagnetic one, in a wide range of concentration ($0 < x \leqslant 0.65$) with maximum $T_N \sim 14$ K, which overlaps with the intermediate valence state of Eu existing in the full range of concentration [13] x [137]. In addition, clear evidence of the formation of the heavy fermion state in the concentration range $0.7 < x < 0.8$ have been presented in [131]. A further increase in the Si-concentration up to the complete substitution for Ge results in the formation of the specific intermediate valence ground state with a spin gap [138, 132] which, upon increasing the temperature above 100 K, transforms into the state with strong spin fluctuations (for $EuCu_2Si_2$, the value $\Gamma_{QE}/2 \geqslant 120$ K has been fixed). The metallic behavior is specific for the system for any x value.

It should be noted that spectra of magnetic response demonstrate quite remarkable temperature evolution in the concentration range $0.7 < x < 1.0$ [132, 135], (Fig. 28, Fig. 29), and a very important peculiarity of low temperature spectra is the absence of any evidence of spectral features specific to Eu^{2+} or Eu^{3+}. As is known for the Eu^{2+}-configuration ($4f^7$) in the paramagnetic state, an intensive ($\sigma_{mag} = 38.5$ barn) quasielastic response with a temperature dependent width and for Eu^{3+} ($4f^6$) a specific intermultiplet transition at the energy of 45 meV ($\sigma_{mag} = 7.4$ barn) are expected.

A peculiar property of magnetic excitation spectra is the existence of two peaks in its inelastic part with the specific characteristics (form factors, temperature dependence of the energies and intensities (see Fig. 29) indicating some difference in its physical origin. As is shown in [132], its energies are systematically dependent on the average valence but by a different power law (Fig. 30); the intensity of the peak with higher energy (Ex2) is in full correspondence (Fig. 29b) with the expected one for spin-orbital transition $^7F_0 - ^7F_1$ of Eu^{3+} normalized to the average valence. Thus, the $^7F_1$ CEF-splitting origin can not be considered a source of the double peak structure, even hypothetically. The above conditions allow us to suggest that peak Ex2 corresponds to the renormalized spin-orbital excitation related to the transition $J = 0 - J = 1$ ($^7F_0 - ^7F_1$) for Eu^{3+}, but the peak Ex1 represents a resonance mode related to the excitation from the true ground state of the quantum mechanically mixed wave function of intermediate valence europium, in analogy with SmB_6 or Sm(Y)S (see above, Section 3.2.2).

Results of detailed studies of the valence state by X-ray spectroscopic (L_3-edge XANES) and by nuclear resonance

[13] It was established earlier that copper ions do not carry any magnetic moment in this compound.

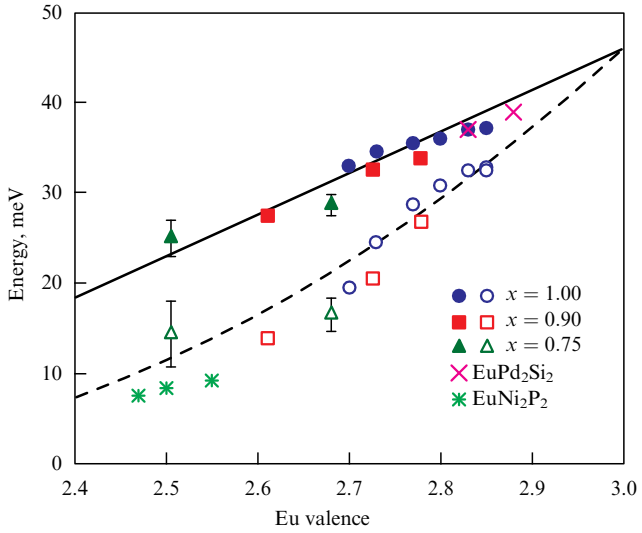

Figure 30. Dependences on the Eu valence for the energy of the inelastic peaks for $EuCu_2(Si_xGe_{1-x})_2$: (Ex1 — unfilled symbols and Ex2 — filled ones), for $EuPd_2Si_2$ and $EuNi_2P_2$. (Data taken from [132].) Symbols of different types correspond to different compositions and temperatures. Lines — model calculation as explained in [132]. Extrapolation to valence value 3+ results in coincidence of the energies of both peaks at about 45 meV, consistent with the energy of spin-orbital excitation for Eu^{3+}. Values for energies of inelastic peaks of $EuPd_2Si_2$ and $EuNi_2P_2$ are taken from [139] and [140], respectively, valence values of Eu are taken from [141, 142].

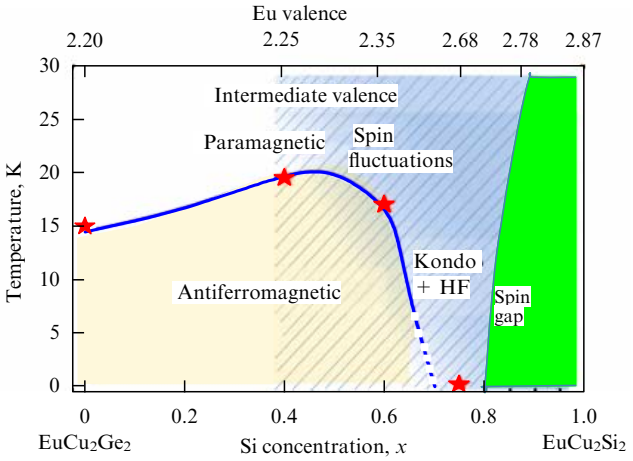

Figure 31. Magnetic phase diagram for $EuCu_2(Si_xGe_{1-x})_2$, based on thermodynamic data [131] (solid blue line) and subsequent neutron study results [133–135]. Stars denote the values of T_N obtained from neutron diffraction experiments [133]. The region on the right in green corresponds to the regime of spin-gap for the ground state; the hatched area corresponds to the experimentally observed spin fluctuations which manifest themselves as quasielastic peak in neutron spectra. The values of the valence on the top scale correspond to the temperature region below 30 K according to the data of [132]. (Data taken from [135].)

(isomer shift in the Mössbauer effect) methods, long range magnetic order, and spectral features by thermal neutron scattering and mutual correlations of these data are discussed in [133–135]. The main results are as follows.

Valence of europium is different from the integer number for the full range of x, from $EuCu_2Ge_2$ up to $EuCu_2Si_2$, with a variation from 2.2 to 2.85 ($T = 5$ K). The mixed valence state of Eu appears to be homogeneous, meaning there is no spatial separation into 2+ and 3+ ions. Nevertheless, it is necessary here to take note, because there is no consensus in the literature with respect to reliability of the quantitative estimation of Eu-valence close to the 2+ value when measured by XANES or Mössbauer spectroscopy. Without going into the technical details of possible parasitic effects, we should note that in the present particular case a number of arguments exist which allow us to consider the region of concentration $0.4 < x < 1.0$ as corresponding to the IV state of Eu at least. As concerns the lower x values, up to 0, there are some reasons to treat the valence as close to 2+, but our estimation of the variety of the available data allows us to be consistent with the results presented in [133–135] mentioned above.

Long range magnetic order is shown to be antiferromagnetic with a propagating vector $\mathbf{k} = (1/3, 0, 0)$. An ordered magnetic moment does not reach a maximum value specific for the Eu^{2+} in the whole range of compositions, progressively decreasing with increasing Si concentration. The Néel temperature at the same time changes nonmonotonically, as was first established in [131], attaining the maximum value at about $x = 0.5$, and then sharply drops to zero. The sequence of the ground states is presented in the diagram in Fig. 31.

There is a relatively large concentration range, from approximately $x = 0.4$ up to $x = 0.65$, where LRMO coexists with spin fluctuations which do not exceed the thermal limit (similarly to magnetic HF systems (see Section 3.4.1); such co-existence has not been observed for the TmSe IV system.

The most surprising fact is the combination of the maxima of the noninteger valence value (about 2.5) realized for a concentration x region of approximately 0.65–0.75, with the heavy fermion ground state specific to the corresponding area of the phase diagram close to the border with the AF LRMO region. In fact, the HF state of Eu is formed on the basis of the spin-gap (spin-fluctuative at high temperatures) state following an increase in the extent of intermediate valence starting from $x = 1$ with valence 2.85. Contrary to this, for cerium and ytterbium systems the HF state is realized for small deviations of the valence from integer values (3+) and is described by the Kondo model representation, which means under the assumption of a perturbation theory with weak hybridization. It is necessary to note that the HF state has not been observed at all for the case of TmSe with a high extent of intermediate valence quite similar to that observed at the border of the LRMO state in $EuCu_2(Si_xGe_{1-x})_2$.

Apparently, the experimental 'key' for an understanding of the origin of this unusual and new phenomenon is the analysis of concentration (x) dependence (in fact, concentration Si/Ge defines the valence of Eu) for parameters of the magnetic excitation spectrum, in particular, the correspondence of the parameters of the quasielastic spectral component (always existing at high temperatures) and inelastic excitations with Eu-valence (Fig. 32). Indeed, for $0.75 < x < 1.00$ and high enough temperatures, the width of a quasielastic peak is substantially larger than that typical for HF ones (compare with Fig. 24), in spite of the fact that at low temperatures the quasielastic scattering is absent (which means the ground state is a nonmagnetic singlet). The energy of inelastic peaks for this concentration range is high enough, gradually decreasing with a decrease in x from 1 to 0.8. When x decreases to 0.75, the width and energy of inelastic peaks come to comparable values; moreover, a quasielastic peak exists at any temperature and its width is not so large, coming close to typical values of HF systems.

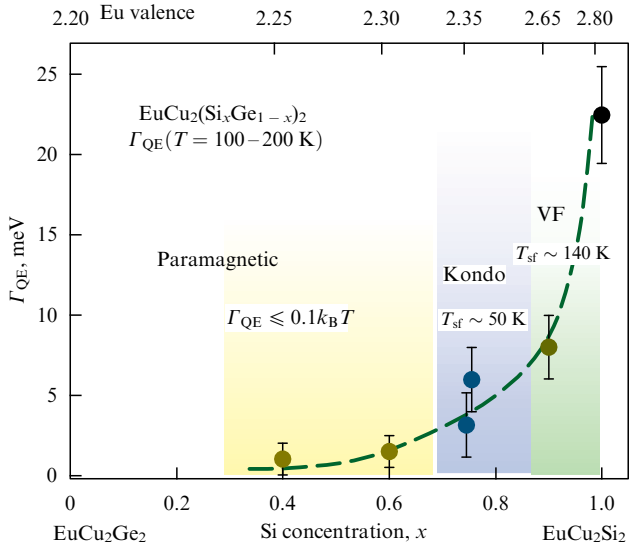

Figure 32. Concentration dependence of the width of the quasielastic peak (FWHM) for a series of samples $EuCu_2(Si_xGe_{1-x})_2$ in the intermediate temperature range (100–200 K). Top scale — Eu-valence for appropriate temperatures. Color selection corresponds to: intermediate valence state with spin gap ground state (VF, green); Kondo-regime with heavy fermion ground state (Kondo, violet); spin-fluctuative regime in paramagnetic state and LRMO at low temperatures (yellow). (Taken from [135].)

Finally, an excitation spectrum similar to the one characteristic of the 'classical' HF system (see above, Section 3.1) is formed on strengthening the intermediate valence by decreasing the silicon concentration x. A further decrease in x (below $x = 0.7$) is accompanied by a further decrease in quasielastic width and, in this sense, the formation of the necessary conditions for the transition to the LRMO ground state, in analogy with magnetic HF systems. This scenario is bolstered by the presence near the Fermi energy not only of f-type electron states but of other bands formed by electron shells of Cu and Si (Ge), contrary to the case of TmSe, which is an ionic type crystal. A consequence of the same situation is, perhaps, the absence in $EuCu_2Si_2$ of the metal–insulator transition which is typical of 'classical' Kondo insulators. Strong correlations and the formation of a spin gap are not accompanied by the disappearance of metallic conductivity due to the multiband structure near the Fermi level.

It is necessary to mention the principal difference between Eu-based system and TmSe: in spite of the presence of 6 f-electrons, for Eu^{3+} the ground state is the spin-orbital singlet (nonmagnetic state) and it is separated from the excited magnetic triplet by an energy of 45 meV. Therefore, only renormalization of the magnetic excitation spectrum of the real ground state under IV conditions enhanced by decreasing x and the closing of the spin gap produce the conditions for the formation of the spin-fluctuative ground state with some magnetic moment.

There are not too many theoretical approaches describing a multi-occupied electronic state in IV systems (meaning not f^1 or f^{13}). Besides the publications mentioned above (in connection to TmSe, Section 3.4.2), it is necessary to mention [143], where the 'extended s – f model' is analyzed in relation to early experimental results on Eu-based systems (elemental Eu, $Eu(Pd, Ag)_2Si_2$). In this model, the exchange interaction independent of Kondo-type hybridization is present; therefore, the coexistence of AF LRMO with valence fluctuations appears to be possible. This model predicts the nonmonotonic behavior of T_N as a function of the hybridization parameter, as was observed for the $EuCu_2(Si_xGe_{1-x})_2$ series. Unfortunately, the existence of the HF regime in the case of $EuCu_2(Si_xGe_{1-x})_2$ excludes this mechanism from consideration, due to the positive value of the s – f interaction constant intrinsic to the model [143]. It is necessary to mention recent paper [144] which considers the multi-occupied f-shell as some intermediate case of the L – S and j – j type of coupling, which allows the Kondo-regime for the Eu^{2+} state to be obtained under some conditions.

3.4.4 Magnetic Kondo insulators: 1 – 2 – 10-type Ce-based systems CeM_2Al_{10} (M = Fe, Ru, Os). The development of research on the properties of a new class of Ce-based systems with the formula CeM_2Al_{10} (M = Fe, Ru, Os) (below as 1–2–10) substantially enriched in recent years the physics of Kondo insulators with new unusual and interesting facts.

From the structural point of view, these compounds with orthorhombic symmetry (Cmcm — type) of crystal lattice (Fig. 33) seems to be partly similar to hexa- and dodecaborides in the sense that the RE ion is localized inside the 'cluster' (polyhedron) formed by Al and T-type atoms; due to this fact, the distance Ce–Ce is fairly large, about 5.2 Å [145].

There seem to be no grounds to expect quite strong interaction of magnetic moments of RE ions; in fact, for the isostructural compound $GdRu_2Al_{10}$ based on Gd — an RE ion with much higher magnetic moment than Ce: around $7\mu_B$ — the Néel temperature does not exceed 18 K (no ordering in d-element sublattice is found for this type of compound). Nevertheless, in a related Ce-based compound T_N appears to be about 27 K (see Fig. 34), and for $CeOs_2Al_{10}$ it is even higher — $T_N = 29$ K. Only $CeFe_2Al_{10}$ is paramagnetic down to temperatures below 1 K [147, 148].

Looking at the Gd-concentration dependence of the ordering temperature shown in Fig. 34, one can suppose that different physical mechanisms are responsible for the magnetic ordering of Ce-based and Gd-based sublattices. This follows from the fact that an increase in the concentration of Gd with a much larger magnetic moment than the one of Ce in $Ce_{1-x}Gd_xRu_2Al_{10}$ results in a sharp drop in the ordering temperature and only after that to some gradual increase at the Gd-rich end of the phase diagram.

Experiments show that, above the ordering temperature for all three systems, maxima of the magnetic susceptibility

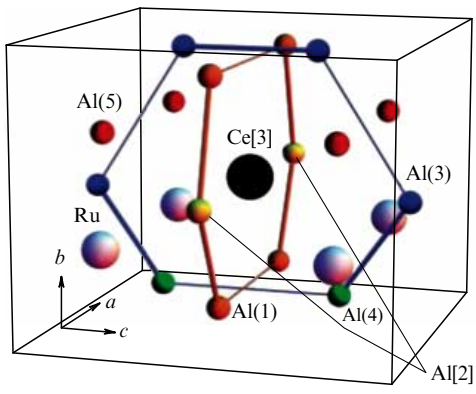

Figure 33. Unit cell for $CeRu_2Al_{10}$ compound indicating atomic location (from [146]). Positions of Al [2] are specified, apparently, due to effects of hybridization interaction (see below).

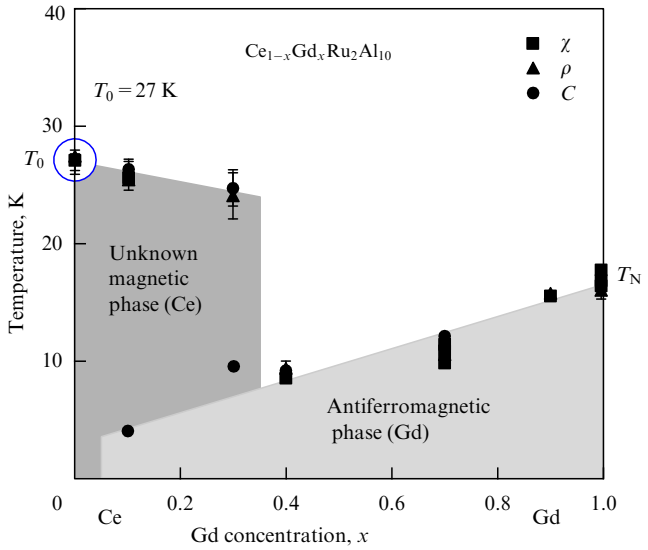

Figure 34. Magnetic phase diagram for system $Ce_{1-x}Gd_xRu_2Al_{10}$ from paper [150]. Different symbols denote the temperatures of transition to the magnetically ordered state defined from measurements of magnetic susceptibility (χ), electrical conductivity (ρ), and heat capacity (C).

[147, 148] (see Fig. 35), an exponential increase in the electric resistance, evidence of high electron density at the Fermi-level [150, 151] is observed. Besides this, L_3-edge spectra of X-ray absorption for $CeFe_2Al_{10}$ demonstrate the noninteger valence of cerium [152]. Thus, all the 1–2–10 systems present evidence of an aggregate of properties typical of Kondo insulators, corresponding to the possibility of the formation of charge and spin gaps on a further decrease in the temperature. Moreover, the measurements of the conductivity of $CeRu_2Al_{10}$ under pressure [151] have shown that under growing pressure the gap in electron density of states develops at 2 GPa, which further collapses, and above 4 GPa the metallic (and paramagnetic) state develops.

The formation of AF LRMO in $CeOs_2Al_{10}$ and $CeRu_2Al_{10}$ is a fool-proof fact based on data from neutron diffraction on powder and single crystals, as well [153, 154]. It is surprising that, from the neutron studies [155, 156], a very low value ($\sim 0.3\ \mu_B$) of the magnetic moment in the Ce ion has been established, and its orientation along the c-axis does not coincide with the easy axis a resulting from the anisotropy of the magnetic susceptibility in a large range of temperatures. Thus, the orientation and magnitude of the magnetic moments are not consistent with the magnetic anisotropy of the paramagnetic state of a crystal and its quite high ordering temperature as well.

Spectra of magnetic excitation have been studied in poly- and single crystal samples of these compounds [153, 157–159] focusing on the structure of the spectra (for Kondo insulators, characteristic features could be indicated) and the details of its temperature evolution, in particular, in connection with magnetic phase transition. Measurements with time-of-flight spectrometers with poly-crystal samples in a wide range of energy transfers and temperatures have been done. They show that the spectrum of magnetic excitations is characterized by the presence of a quite narrow peak at low energy transfer: 8–10 meV for $CeOs_2Al_{10}$ (see Fig. 36) and for $CeRu_2Al_{10}$ (see Fig. 37a), and 10–14 meV for $CeFe_2Al_{10}$ (see Fig. 37b).

These peaks practically disappear above T_N or the temperature maximum for static magnetic susceptibility (for $CeFe_2Al_{10}$), being replaced by a quasielastic signal with a width of the order of a few meV, as seen from Fig. 37. Along with this clear peak, some area of magnetic scattering without a pronounced spectral structure continuing up to a few dozen meV has been observed, which apparently can be related to deeply damped magnetic excitations.

Detailed measurements with a single crystal on three-axis spectrometers, including the option of polarization analysis, have allowed us to get the structure of the low energy excitation spectrum and to study its temperature evolution. For $CeRu_2Al_{10}$ [158], it was established, in particular, that in the range of 5–8 meV two excitations with dispersion exist, and its energy maxima are at the center of the crystal Brilluoin zone, that is, in accordance with the AF type of magnetic correlations. The existence of two excitations is in agreement with the number of Ce ions (just two) in the primitive structure cell. An increase in the temperature results in a decrease in the energy of excitations [153, 157] (Fig. 37b), as expected for the antiferromagnetic type of spectrum with a spin-gap in the magnetic zone center.

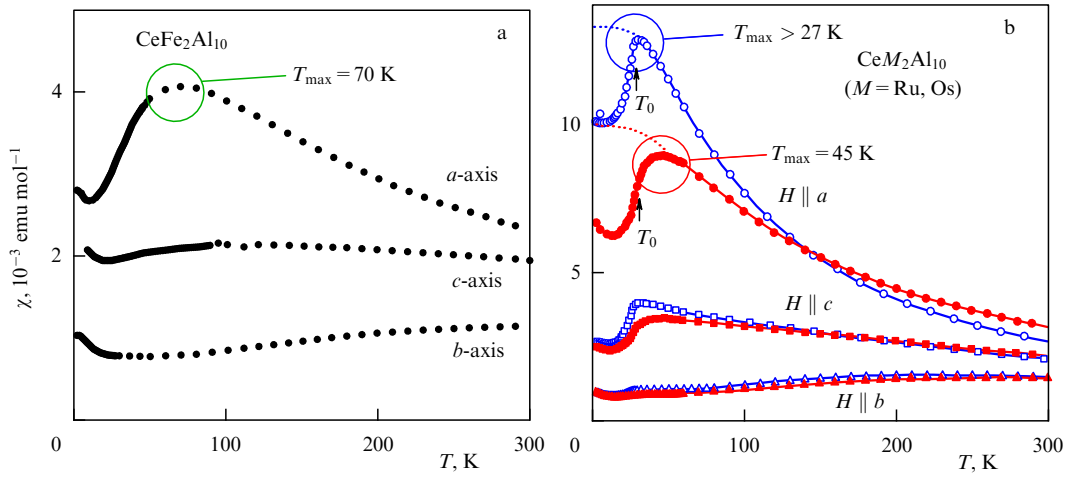

Figure 35. Anisotropy of magnetic susceptibility measured for CeM_2Al_{10} single crystals [147, 148]. Circles denote the temperature positions of the maxima of magnetic susceptibility, arrows show the temperatures of magnetic phase transition T_0 (below the temperatures corresponding to positions of maxima).

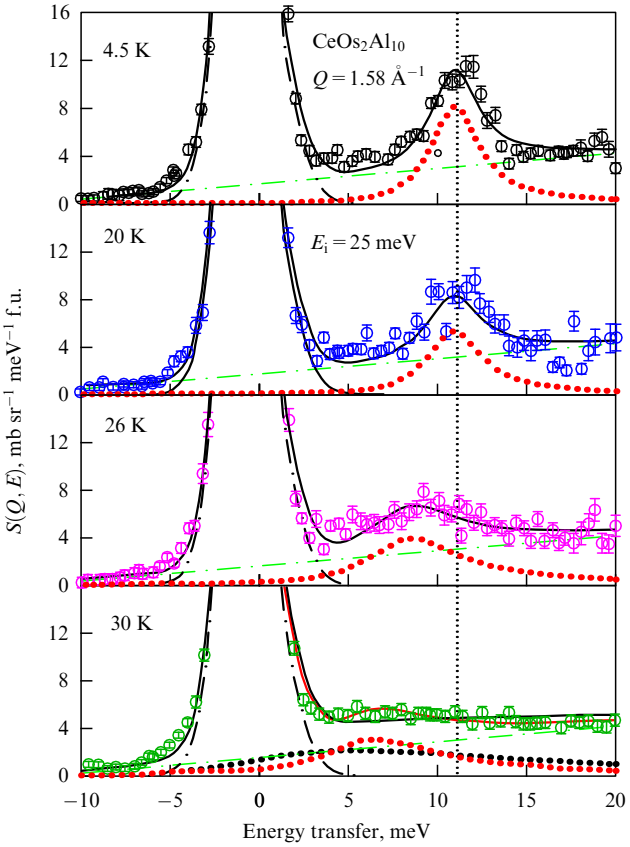

Figure 36. Temperature dependence of the inelastic neutron scattering spectrum measured for poly-crystal sample $CeOs_2Al_{10}$ at low neutron momentum transfer (initial neutron energy of 25 meV) that corresponds to domination of magnetic contribution to the scattering function (from [157]). The peak related to magnetic excitation is shown by the (red) dotted line; the vertical line allows an estimate of the temperature driven shift of the peak energy (see text).

The character and features of the dispersion of energy and intensity for two observed low energy modes are reasonably well reproduced by the calculations using the phenomenological model of anisotropic exchange interaction in the mean field approximation for antiferromagnetic magnons. This model provides a right orientation of magnetic moments in the ordered state but only in assumption that exchange constant along c appears to be many times larger than for others directions [158]. This immediately results in the increase of the calculated value of magnetic moment in three times over the experimental one [155, 156]. The latter may be reproduced in one's turn, by the calculation of the crystal field splitting, taking into account the experimental result of balk susceptibility measurements (the easy axis as *a*) in paramagnetic state. Thus, it is clear that for the case of such magnetic Kondo-insulator simple combination of a crystal field and an exchange interaction does not work for the attempt to describe magnetic properties of single-ion and cooperative states by unified physical approach, even if to forget about the problem of too much high T_N.

The $CeFe_2Al_{10}$ doesn't demonstrate LRMO and is much less 'disputed' in the sense of physical properties, showing good correspondence with the typical Kondo insulator as YbB_{12}. Experiments with single crystal at TAS [159] allowed to study in details a structure of low energy part of magnetic excitation spectra of $CeFe_2Al_{10}$. In fact, below the 50 K a spin-gap is present of 15 meV range in the spectrum, this means absence of the any evidence of spin-fluctuations in the form of quasielastic spectral contribution. Resonance mode (at 10 meV, Fig. 37c) has a dispersion of AF-type, but with principal difference with respect to the case of ordered $CeRu_2Al_{10}$. Increase of the temperature is, as usual, suppressing the dispersion of excitation but its energy is not decreasing as in case of antiferromagnetic state, on the contrary, its increasing (Fig. 37c), coming to the gap border, as it is predicted for the excitation of spin-exciton type in paramagnetic state [160]. Anisotropy of the intensity of this peak corresponds to the single-ion behavior.

It could be assumed that $CeFe_2Al_{10}$ represents a typical Kondo insulator when taking into account anisotropy and the presence of two magnetic ions in a primitive cell.

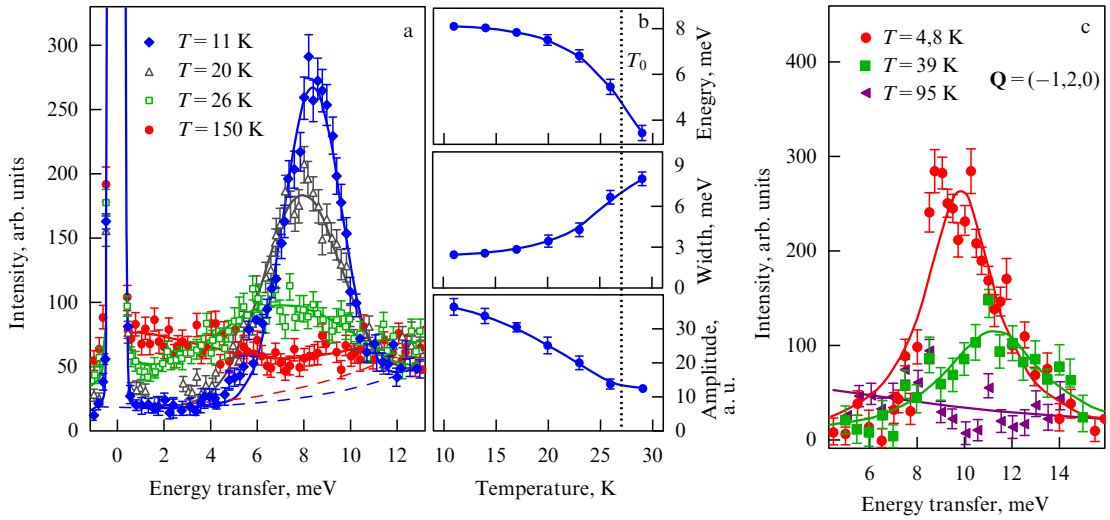

Figure 37. (Color online.) Temperature dependences of the parameters of low-energy magnetic excitation for $CeRu_2Al_{10}$ (from [153]) and a single crystal sample of $CeFe_2Al_{10}$ (from [159]). (a) Spectra for polycrystalline $CeRu_2Al_{10}$ measured with three-axis spectrometer with fixed final energy $E_f = 5$ meV. Temperature dependences (b) for energy of the peak, its width at half maximum (FWHM), and amplitude in the $CeRu_2Al_{10}$ spectrum. (c) Spectra for the single crystal of $CeFe_2Al_{10}$ measured with three-axis spectrometer with fixed final energy $E_f = 14.7$ meV at the center of the magnetic Brillouin zone (−1, 2, 0) where the maximum of the peak intensity is observed. This zone is identical to the magnetic zone obtained for $CeRu_2Al_{10}$.

Alternatively, two other compounds need to be considered, taking into account extra physical interactions for the explanation of the observed specifics of the magnetic behavior. The first idea related to this issue is the possible role of hybridization [146] in the formation of the anisotropy of f–c electron interaction, in particular, the existence of a strong hybridization component along axis *a* arising from interaction Ce–Al [2], as shown in Fig. 33. Another essential factor is related to the proximity of these systems, as supposed in [161], to the border of the crossover from the localized to the itinerant magnetic case (the itinerant character grows upon moving from Ru to Os and Fe in the series).

4. Conclusion. Role of neutron spectroscopy in the development of physical concepts on the origin of unusual properties of systems with correlated electrons

This review presents a number of interesting and important experimental results which demonstrate specific features of SCES physics (of course this is a subjective choice, obviously without claiming to be all-embracing). Nor, in fact, did we go deeply into theoretical aspects of physical models which were developed simultaneously with experimental activity: this evidently would result in the unacceptable overloading of this publication for the given format.

In summary, below, the main physical results will be formulated obtained owing to the development of the inelastic neutron scattering study of SCES starting from the middle of the 1970s. Along with this, based on recent and current research presented in the review as examples of unique possibilities of the neutron spectroscopy method for accomplishing the task of studying the fundamental background for the unusual physical property formation in this class of systems, we will point out a number of problems to be analyzed and solved in the future.

(1) Systematic experimental studies underpinned the conception of the crystal field in metals to be considered as an essential factor of the formation of the physical properties in systems with localized moments of spin-orbital origin. It was established that symmetry properties of the CEF potential are determined by the nearest crystal surrounding of the magnetic ion, and crystal symmetry serves as a basis for the phenomenological description of CEF effects in the metallic state. Conduction electrons play a very important role in the formation of the crystal field potential. A considerable part of these results has been obtained in our country with neutron spectrometers in the Condensed Matter Physics and Superconductivity Department at the I V Kurchatov Institute of Atomic Energy (now the National Research Centre 'Kurchatov Institute') and the I M Frank Laboratory for Neutron Physics at the Joint Institute for Nuclear Research in the 1970s and 1980s. The further development of neutron spectroscopy studies of SCES, in particular, due to the efforts of scientists in the Urals (Institute of Metal Physics of Ural Branch of the RAS), has been closely related to support from the grant program of the Russian Foundation for Basic Research and international scientific collaboration as well.

(2) The model of induced long range magnetic order with phase transitions driven by the 'soft mode', based on the ideas of the polarization mechanism for magnetism formation in singlet ground state systems, has received experimental confirmation due to the study of the systems with low symmetrical CEF potential.

(3) The sensitivity of CEF effects to structural and charge characteristics of local surroundings allowed the study of fine details of spatially inhomogeneous states in HTSC. Such an approach serves as an important complementary source of information about the specifics of local atomic and electronic structure, which is usually extracted from X-ray spectroscopy methods such as XAFS (see, for instance, [162, 163]). This complementarity is of great importance for the understanding of the microscopic origin of superconductivity in copper oxide-based SCES. In the further development of neutron studies of SCES, the accent is shifted considerably to the side of dynamics of 'anomalous' systems which demonstrate unusual physical properties with respect to 'ordinary' intermetallics with local magnetic moments.

(4) The study of heavy fermion systems, first of all, 'classical' compounds like $CeAl_3$, $CeCu_2Si_2$, and others, allowed establishing microscopic features of the Kondo-effect as an dynamical effect of screening of the local magnetic moment. An estimate of the characteristic energy of spin fluctuations for the bonded state of the localized f-moment with spin of conduction electrons has been obtained. It also was shown that this 'screening' has nothing to do with redistribution of charge density in the crystal, but contributes to the renormalization of the energies and structure of wave functions for CEF levels of the Kondo ion. Apparently, these effects originate from hybridization. The characteristic temperature of the above transformation for dynamical magnetic response corresponds to the scale of CEF splitting. It is important to note that the local magnetic moment itself doesn't disappear when the temperature goes to zero, keeping almost its full value.

(5) Comprehensive studies have been carried out of dynamical effects in magnetic and lattice subsystems of 'classical' intermediate valence compounds based on Sm: SmB_6 and $Sm_{1-x}Y_xS$. The formation of the nonmagnetic singlet ground state separated by a gap from the continuum of magnetic excitations has been discovered. The 'resonance' magnetic mode discovered at low temperatures has been studied; it was related to the excitation spectrum of the partially delocalized f-electron state due to a clear relation between the valence and resonance mode energy and the form factor. An important feature of the electron–phonon interaction in these systems was discovered experimentally, namely the resonance violation of the adiabatic approximation. All these as well as a number of other effects, are caused by the presence of low energy spin and charge excitations in the spectra of the new intermediate valence state realized in each RE ion.

(6) A qualitatively similar picture (spin gap, in-gap magnetic modes, phonon anomalies in lattice dynamics, etc.) has been established in a series of publications devoted to neutron spectroscopy studies of metallic intermediate valence compounds based on CeNi. An important feature of this IV substance is the formation of a spin gap (that is, total suppression of the quasielastic component in the spectrum of magnetic response upon decreasing temperature) combined with an undamaged metallic state. Apparently, a possible prerequisite of such phenomena is a relatively complicated band structure near the Fermi level related to the low local symmetry and a more complicated crystal structure. Along with these results obtained, the role of local vs cooperative effects in the substance still needs further investigation and analysis.

(7) A series of comprehensive publications related to the coupling and competition of nonuniformly scaled interactions in the prototypical Kondo insulator YbB_{12} — 3D-cluster-network system with related metal–insulator transitions and paramagnet–nonmagnetic states was carried out. The resonance mode existing in the spin gap, anomalies in lattice dynamics which are related to the formation of the nonmagnetic and insulating ground state, the relation of these features to hybridization, and exchange and crystal field effects have been demonstrated and studied.

(8) Systematic studies have been conducted of the intermediate valence system based on Eu, $EuCu_2(Si, Ge)_2$, which is to date the only known system with a combination of IV behavior with a sequence of ground states like spin-gap, heavy fermion, LRMO AF. It has been shown that the background of this sequence is the modification of the magnetic excitation spectrum of the IV Eu ion; the problem of an adequate model has been formulated. A similar problem — the search for adequate physical models — appears to be quite relevant for new magnetic Kondo insulators of the series CeM_2Al_{10} (M = Fe, Ru, Os — d-metals)

It is clear that experimental results obtained for Kondo insulator and, Ce-, Eu-based IV and HF systems, such as the discovery and quantitative characterization of spin-fluctuations, spin gap, and other features of the excitation spectra (resonance mode, etc.) are very important achievements in physics provided by the unique possibilities of the neutron scattering method. The data obtained can not be identified as corresponding totally to local or cooperative considerations. Its understanding requires the development of more appropriate theoretical models (in particular, to describe combination of magnetic ordering with the heavy fermion state and valence fluctuations, identify a source of cooperative effects in Kondo insulator, and so on). It is necessary to mention that the existence of the resonance mode discovered in the discussed class of systems is characteristic for copper-oxide-based and iron-pnictides-based HTSC, as well as for RE-based and actinide-based heavy fermion superconductors. Thus, the spectral characteristics provide some evidence of a general basis for physical phenomena and corresponding problems.

We consider establishing general regularity in the formation of different types of ground state in solids as a result of the mutual influence of the *principal physical factors*: *CEF — exchange–hybridization*, on the background of intra-atomic interactions responsible for the formation of unfilled electron shells an important element to ensure the building of the generalized models.

In relation to the above, it seems appropriate to develop the study of the considered states and their mutual transformations in a system build-up on the basis of elements from the center of RE series. It is true that for such systems, contrary to systems based on beginning (Ce) or end (Yb) of series, there is a lot less experimental data. This is one of the crucial tasks for neutron-spectroscopy studies at present and in the near future.

The author is deeply grateful to I P Sadikov for ideas on initiation and an invaluable personal contribution to the development of neutron research in this area, to V N Lazukov, A S Ivanov, and A Yu Rumyantsev for their participation and full support of the work, to Yu M Kagan, L A Maksimov and K A Kikoin for their constant and stimulating interest in these studies and the results obtained. A great contribution to our joint work was made by J-M Mignot, A Furrer, R Eccleston, R Bewley, A V Mirmelstein, V G Orlov, E A Goremychkin, A P Menushenkov, O D Chistyakov, N Yu Shitsevalova, V B Filippov, and A V Gribanov. Fruitful creative collaboration with colleagues E V Nefeodova, E S Clementyev, K S Nemkovski, and N N Tiden for many years has enabled us to formulate and solve interesting problems.

The author is grateful for partial financial support from RSF, grant 14-22-00098 (Sections 1, 2, 4 of the publication) and for partial financial support from RFBR, grant 14-02-01002 ofi-m (Section 3 of the publication).

References

1. Marshall W, Lovesey S W *Theory of Thermal Neutron Scattering: the Use of Neutrons for the Investigation of Condensed Matter* (Oxford: Clarendon Press, 1971)
2. Holland-Moritz E, Wohlleben D, Loewenhaupt M *Phys. Rev. B* **25** 7482 (1982)
3. Balcar E, Lovesey S W *Theory of Magnetic Neutron and Photon Scattering* (Oxford: Oxford Univ. Press, 1989)
4. Turberfield K S et al. *Phys. Rev. Lett.* **25** 752 (1970)
5. Taylor K N R, Darby M I *Physics of Rare Earth Solids* (London: Chapman and Hall, 1972); Translated into Russian: *Fizika Redkozemel'nykh Soedinenii* (Moscow: Mir, 1974)
6. Rainford B et al. *J. Phys. C* **1** 679 (1968)
7. Furrer A, Kjems J, Vogt O *J. Phys. C.* **5** 2246 (1972)
8. Furrer A, Warming E *J. Phys. C* **7** 3365 (1974)
9. Alekseev P A et al. *Fiz. Tverd. Tela* **18** 676 (1976)
10. Alekseev P A *Sov. Phys. Solid State* **18** 1466 (1976); *Fiz. Tverd. Tela* **18** 2509 (1976)
11. Loewenhaupt M, Rainford B D, Steglich F *Phys. Rev. Lett.* **42** 1709 (1979)
12. Aksenov V L et al. *J. Phys. F* **11** 905 (1981)
13. Walter U, Holland-Moritz E *Z. Phys. B* **45** 107 (1981)
14. Alekseev P A et al. *Phys. Status Solidi B* **114** 161 (1982)
15. Alekseev P A et al. *Phys. Status Solidi B* **119** 651 (1983)
16. Goremychkin E A, Mühle E *JETP Lett.* **39** 570 (1984); *Pis'ma Zh. Eksp. Teor. Fiz.* **39** 469 (1984)
17. Fulde P, in *Handbook on the Physics and Chemistry of Rare Earths* Vol. 2 (Eds K A Gschneidner (Jr.), L Eyring) (Amsterdam: North-Holland, 1979) p. 295
18. Fulde P, Loewenhaupt M *Adv. Phys.* **34** 589 (1986)
19. Newman D J, Ng B *Rep. Prog. Phys.* **52** 699 (1989)
20. Holland-Moritz E, Lander G H, in *Handbook on the Physics and Chemistry of Rare Earths* Vol. 19 (Eds K A Gschneidner (Jr.), L Eyring) (Amsterdam: Elsevier, 1994) p. 1
21. Furrer A, Podlesnyak A, in *Handbook of Applied Solid State Spectroscopy* (Ed. D R Vij) (New York: Springer, 2006) p. 257
22. Cooper B R, in *Magnetic Properties of Rare Earth Metals* (Ed. R J Elliott) (London: Plenum Press, 1972) p. 17
23. Birgeneau R J, Als-Nielsen J, Bucher E *Phys. Rev. B* **6** 2724 (1972)
24. Mulders A M et al. *Phys. Rev. B* **56** 8752 (1997)
25. Alekseev P A et al. *JETP Lett.* **76** 99 (2002); *Pis'ma Zh. Eksp. Teor. Fiz.* **76** 110 (2002)
26. Tiden N N et al. *Physica B* **378–380** 1085 (2006)
27. Furrer A *J. Supercond. Novel Magn.* **21** 1 (2008)
28. Furrer A et al. *Eur. J. Solid State Inorg. Chem.* **28** 627 (1991)
29. Staub U et al. *Phys. Rev. B* **50** 4068 (1994)
30. Mesot J, Furrer A *J. Supercond.* **10** 623 (1997)
31. Mirmelstein A et al. *J. Phys. Condens. Matter* **11** 7155 (1999)
32. Mirmelstein A et al. *J. Supercond.* **15** 367 (2002)
33. Stewart G R *Rev. Mod. Phys.* **56** 755 (1984)
34. Andres K, Graebner J E, Ott H R *Phys. Rev. Lett.* **35** 1779 (1975)
35. Murani A P et al. *Solid State Commun.* **36** 523 (1980)
36. Murani A P, Knorr K, Buschow K H J, in *Crystal Field Effects in Metals and Alloys. Proc. of the Second Intern. Conf. on Crystal Field Effects in Metals and Alloys, Zürich, Switzerland, September 1–4, 1976* (Ed. A Furrer) (New York: Plenum Press, 1977) p. 268
37. Goremychkin E A, Natkaniec I, Mühle E *Solid State Commun.* **64** 553 (1987)
38. Alekseev P A et al. *Physica B* **217** 241 (1996)

39. Sashin I L, Goremychkin E A, Osborn R *Phys. Solid State* **49** 322 (2007); *Fiz. Tverd. Tela* **49** 311 (2007)
40. Alekseev P A et al. *JETP Lett.* **39** 580 (1984); *Pis'ma Zh. Eksp. Teor. Fiz.* **39** 477 (1984)
41. Alekseev P A, Bührer W *Physica B* **190** 131 (1993)
42. Moshchalkov V V, Brandt N B *Sov. Phys. Usp.* **29** 725 (1986); *Usp. Fiz. Nauk* **149** 585 (1986)
43. Alekseev P A et al. *JETP Lett.* **43** 758 (1986); *Pis'ma Zh. Eksp. Teor. Fiz.* **43** 586 (1986)
44. Kiselev M N, Mishchenko A S *JETP* **86** 1008 (1998); *Zh. Eksp. Teor. Fiz.* **113** 1843 (1998)
45. Newns D M, Hewson A C, in *Valence Fluctuations in Solids. Santa Barbara Institute for Theoretical Physics Conf., Santa Barbara, Calif., January 27–30, 1981* (Eds L M Falicov, W Hanke, M B Maple) (Amsterdam: North-Holland, 1981) p. 27
46. Vainshtein É E, Blokhin S M, Paderno Yu B *Sov. Phys. Solid State* **6** 2318 (1965); *Fiz. Tverd. Tela* **6** 2909 (1964)
47. Hirst L L *Adv. Phys.* **27** 231 (1978); *J. Phys. Chem. Solids* **35** 1285 (1974)
48. Loewenhaupt M, Fischer K H, in *Handbook on the Physics and Chemistry of Rare Earths* Vol. 16 (Eds K A Gschneidner (Jr.), L Eyring) (Amsterdam: North-Holland, 1993) p. 1
49. Lander G H, in *Handbook on the Physics and Chemistry of Rare Earths* Vol. 17 (Eds K A Gschneidner (Jr.), L Eyring) (Amsterdam: North-Holland, 1993) p. 635
50. Wachter P, in *Handbook on the Physics and Chemistry of Rare Earths* Vol. 19 (Eds K A Gschneidner (Jr.), L Eyring) (Amsterdam: Elsevier, 1994) p. 177
51. Holland-Moritz E, Wohlleben D, Loewenhaupt M *Phys. Rev. B* **25** 7482 (1982)
52. Alekseev P A et al. *Physica B* **281–282** 34 (2000)
53. Kikoin K A, Mishchenko A S *JETP* **77** 828 (1993); *Zh. Eksp. Teor. Fiz.* **104** 3810 (1993)
54. Kikoin K A, Mishchenko A S *J. Phys. Condens. Matter* **7** 307 (1995)
55. Alekseev P A et al. *Europhys. Lett.* **10** 457 (1989)
56. Alekseev P A et al. *Physica B* **180–181** 281 (1992)
57. Alekseev P A *Physica B* **186–188** 365 (1993)
58. Mignot J-M, Alekseev P A *Physica B* **215** 99 (1995)
59. Alekseev P A et al. *Europhys. Lett.* **23** 347 (1993)
60. Mignot J-M et al. *Physica B* **199–200** 430 (1994)
61. Alekseev P A et al. *Physica B* **186–188** 384 (1993)
62. Alekseev P A et al. *J. Phys. Condens. Matter* **7** 289 (1995)
63. Boucherle J-X et al. *Physica B* **206–207** 374 (1995)
64. Alekseev P A et al. *Physica B* **259–261** 351 (1999).
65. Alekseev P A et al. *JETP* **81** 586 (1995); *Zh. Eksp. Teor. Fiz.* **108** 1064 (1995)
66. Alekseev P A et al. *J. Solid State Chem.* **133** 230 (1997)
67. Alekseev P A et al. *Physica B* **312–313** 333 (2002)
68. Alekseev P A et al. *Phys. Rev. B* **65** 153201 (2002)
69. Alekseev P A et al. *Phys. Rev. B* **74** 035114 (2006)
70. Alekseev P A et al. *J. Phys. Condens. Matter* **12** 2725 (2000)
71. Alekseev P A et al. *Phys. Met. Metallogr.* **77** 611 (1994); *Fiz. Met. Metalloved.* **77** (6) 60 (1994)
72. Lazukov V N et al. *Europhys. Lett.* **33** 141 (1996)
73. Alekseev P A et al. *JETP Lett.* **63** 1000 (1996); *Pis'ma Zh. Eksp. Teor. Fiz.* **63** 947 (1996))
74. Clementyev E S et al. *Physica B* **234–236** 864 (1997)
75. Clementyev E S et al. *Phys. Rev. B* **57** R8099 (1998)
76. Clementyev E S et al. *Physica B* **259–261** 42 (1999)
77. Clementyev E S et al. *Phys. Rev. B* **61** 6189 (2000)
78. Lazukov V N et al. *Phys. Status Solidi C* **1** 3174 (2004)
79. Alekseev P A *Phys. Usp.* **58** 330 (2015); *Usp. Fiz. Nauk* **185** 353 (2015)
80. Mook H A, McWhan D B, Holtzberg F *Phys. Rev. B* **25** 4321(R) (1982)
81. Mook H A et al. *Phys. Rev. B* **18** 2925 (1978)
82. Holland-Moritz E, Kasaya M *Physica B + C* **136** 424 (1986)
83. Shapiro S M, Birgeneau R J, Bucher E *Phys. Rev. Lett.* **34** 470 (1975)
84. Fuhrman W T et al. *Phys. Rev. Lett.* **114** 036401 (2015)
85. Kuramoto Y, Muller-Hartmann E, in *Valence Fluctuations in Solids. Santa Barbara Institute for Theoretical Physics Conf., Santa Barbara, Calif., January 27–30, 1981* (Eds L M Falicov, W Hanke, M B Maple) (Amsterdam: North-Holland, 1981) p. 139
86. Lazukov V N, Tiden N N, Nemkovski K S "Rol' magnitnykh korrelyatsii v formirovanii spektrov elementarnykh vozbuzhdenii v promezhutochnovalentnom soedinenii CeNi" ("The role of magnetic correlations in the formation of the spectra of elementary excitations in the intermediate-valent compound CeNi"), Preprint IAE-6235/9 (Moscow: Russ. Sci. Center "Kurchatov Institute", 2001)
87. Sujata P et al. *Mod. Phys. Lett. B* **2** 537 (1988)
88. Murani A P et al. *Phys. Rev. B* **48** 10606(R) (1993)
89. Okamura H et al. *Phys. Rev. B* **58** R7496 (1998)
90. Iga F, Shimizu N, Takabatake T *J. Magn. Magn. Mat.* **177–181** 337 (1998)
91. Nefeodova E V et al. *Phys. Rev. B* **60** 13507 (1999)
92. Riseborough P S *Adv. Phys.* **49** 257 (2000)
93. Aeppli G, Fisk Z *Comments Condens. Matter Phys.* **16** 155 (1992)
94. Adroja D T et al. *Optoelectron. Adv. Matter* **10** (7) 164 (2008)
95. Bouvet A et al. *J. Phys. Condens. Matter* **10** 5667 (1998)
96. Alekseev P A et al. *Phys. Rev. B* **63** 064411 (2001)
97. Alekseev P A et al. *J. Phys. Condens. Matter* **16** 2631 (2004)
98. Mignot J-M et al. *Phys. Rev. Lett.* **94** 247204 (2005)
99. Nemkovski K S et al. *Phys. Rev. Lett.* **99** 137204 (2007)
100. Nemkovski K S et al. *Phys. Procedia* **42** 18 (2013)
101. Nemkovski K S et al. *Phys. Solid State* **52** 936 (2010); *Fiz. Tverd. Tela* **52** 878 (2010)
102. Nemkovski K S et al. *Phys. Rev. B* **81** 125108 (2010)
103. Alekseev P A et al. *Phys. Rev. B* **89** 115121 (2014)
104. Rybina A V et al. *J. Phys. Conf. Ser.* **92** 012074 (2007)
105. Alekseev P A et al. *J. Phys. Condens. Matter* **24** 205601 (2012)
106. Liu S H *Phys. Rev. B* **63** 115108 (2001)
107. Akbari A, Thalmeier P, Fulde P *Phys. Rev. Lett.* **102** 106402 (2009)
108. Barabanov A F, Maksimov L A *Phys. Lett. A* **373** 1787 (2009)
109. Rybina A V et al. *Phys. Rev. B* **82** 024302 (2010)
110. Chen G F et al. *Phys. Rev. Lett.* **100** 247002 (2008)
111. Izyumov Yu A, Kurmaev E Z *Phys. Usp.* **51** 1261 (2008); *Usp. Fiz. Nauk* **178** 1307 (2008)
112. Knopp G et al. *J. Magn. Magn. Mater.* **76–77** 420 (1988)
113. Grier B H et al. *J. Phys. C* **21** 1099 (1988)
114. Severing A et al. *Physica B* **163** 409 (1990)
115. Aeppli G, Broholm C, in *Handbook on the Physics and Chemistry of Rare Earths* Vol. 19 (Eds K A Gschneidner (Jr.), L Eyring) (Amsterdam: Elsevier, 1994) p. 123
116. Severing A, Holland-Moritz E, Frick B *Phys. Rev. B* **39** 4164 (1989)
117. Severing A et al. *Phys. Rev. B* **39** 2557 (1989)
118. Doniach S *Physica B + C* **91** 231 (1977)
119. Bucher E et al. *Phys. Rev. B* **11** 500 (1975)
120. Møller H B, Shapiro S M, Birgeneau R J *Phys. Rev. Lett.* **39** 1021 (1977)
121. Launois H et al. *Phys. Rev. Lett.* **44** 1271 (1980)
122. Furrer A, Bührer W, Wachter P *Solid State Commun.* **40** 1011 (1981)
123. Loewenhaupt M, Holland-Moritz E *J. Appl. Phys.* **50** 7456 (1979)
124. Mazzaferro J, Balseiro C A, Alascio B *Phys. Rev. Lett.* **47** 274 (1981)
125. Alascio B et al., in *Valence Instabilities. Proc. of the Intern. Conf., Zürich, Switzerland, April 13–16, 1982* (Eds P Wachter, H Boppart) (Amsterdam: North-Holland, 1982) p. 493
126. Schlottmann P, Falicov L M *Phys. Rev. B* **23** 5916 (1981)
127. Holland-Moritz E *J. Magn. Magn. Mater.* **38** 253 (1983)
128. Greir B H, Shapiro S M, in *Valence Fluctuations in Solids. Santa Barbara Institute for Theoretical Physics Conf., Santa Barbara, Calif., January 27–30, 1981* (Eds L M Falicov, W Hanke, M B Maple) (Amsterdam: North-Holland, 1981) p. 325
129. Mignot J-M, Alekseev P A *Physica B* **215** 99 (1995)
130. Fedro A J, Sinha S K, in *Valence Fluctuations in Solids. Santa Barbara Institute for Theoretical Physics Conf., Santa Barbara, Calif., January 27–30, 1981* (Eds L M Falicov, W Hanke, M B Maple) (Amsterdam: North-Holland, 1981) p. 329
131. Hossain Z et al. *Phys. Rev. B* **69** 014422 (2004)
132. Alekseev P A et al. *J. Phys. Condens. Matter* **24** 375601 (2012)
133. Alekseev P A et al. *JETP Lett.* **99** 164 (2014); *Pis'ma Zh. Eksp. Teor. Fiz.* **99** 185 (2014)
134. Alekseev P A et al. *Phys. Procedia* **71** 303 (2015)
135. Nemkovski K S et al. *Phys. Rev. B* **94** 195101 (2016)
136. Levin E M et al. *Phys. Status Solidi B* **161** 783 (1990)
137. Fukuda S et al. *J. Phys. Soc. Jpn.* **72** 3189 (2003)

138. Alekseev P A et al. *JETP* **105** 14 (2007); *Zh. Eksp. Teor. Fiz.* **132** 22 (2007)
139. Holland-Moritz E et al. *Phys. Rev. B* **35** 3122 (1987)
140. Holland-Moritz E et al. *Z. Phys. B* **77** 105 (1989)
141. Wortmann G et al. *J. Magn. Magn. Mater.* **49** 325 (1985)
142. Perscheid B, Sampathkumaran E V, Kaindl G *J. Magn. Magn. Mater.* **47–48** 410 (1985)
143. Bulk G, Nolting W *Z. Phys. B* **70** 473 (1988)
144. Hotta T *J. Phys. Soc. Jpn.* **84** 114707 (2015)
145. Muro Y et al. *J. Phys. Soc. Jpn.* **78** 083707 (2009)
146. Hanzawa K *J. Phys. Soc. Jpn.* **79** 084704 (2010)
147. Kondo A et al. *Phys. Rev. B* **83** 180415(R) (2011)
148. Takesaka T et al. *J. Phys. Conf. Ser.* **200** 012201 (2010)
149. Kobayashi R et al. *J. Phys. Soc. Jpn. Suppl.* **80** SA044 (2011)
150. Strydom A M *Physica B* **404** 2981 (2009)
151. Nishioka T et al. *J. Phys. Soc. Jpn.* **78** 123705 (2009)
152. Adroja D T et al. *Phys. Rev. B* **87** 224415 (2013)
153. Robert J et al. *Phys. Rev. B* **82** 100404(R) (2010)
154. Mignot J-M et al. *J. Phys. Soc. Jpn. Suppl.* **80** SA022 (2011)
155. Khalyavin D D et al. *Phys. Rev. B* **82** 100405(R) (2010)
156. Kato H et al. *J. Phys. Soc. Jpn.* **80** 073701 (2011)
157. Adroja D T et al. *Phys. Rev. B* **82** 104405 (2010)
158. Robert J et al. *Phys. Rev. Lett.* **109** 267208 (2012)
159. Mignot J-M et al. *Phys. Rev. B* **89** 161103(R) (2014)
160. Riseborough P S *J. Magn. Magn. Mater.* **226–230** 127 (2001)
161. Hoshino S, Kuramoto Y *Phys. Rev. Lett.* **111** 026401 (2013)
162. Menushenkov A et al. *Z. Kristallog.* **225** (11) 487 (2010)
163. Menushenkov A P et al. *J. Supercond. Novel Magn.* **27** 925 (2014)